

Optical spectrum of the post-AGB star HD 56126 in the region 4010–8790 Å

V.G. Klochkova¹, E.L. Chentsov¹, N.S. Tavganskaya¹, and M.V. Shapovalov²

¹ Special Astrophysical Observatory RAS, Nizhnij Arkhyz, 369167 Russia,

² Rostov State University, Rostov-on-Don, Russia

October 23, 2018

Abstract We studied in detail the optical spectrum of the post-AGB star HD 56126 associated with the IR-source IRAS 07134+1005. We use high resolution spectra ($R = 25000$ and 60000) obtained with the echelle spectrographs of the 6-m telescope. About one and a half thousand absorptions of neutral atoms and ions, absorption bands of C_2 , CN, and CH molecules, and interstellar bands (DIBs) are identified in the 4010 to 8790 Å wavelength region, and the depths and radial velocities of these spectral features are measured. Differences are revealed between the variations of the radial velocities measured from spectral features of different excitation. In addition to the well-known variability of the $H\alpha$ profile, we found variations in the profiles of a number of Fe II, Y II, and Ba II lines. We also produce an atlas* of the spectrum of HD 56126 and its comparison star α Per.

1. Introduction

The star HD 56126 is observed in the post-AGB phase of its evolution. While undergoing this short-lived stage (according to Blöcker [1], this phase lasts for $\Delta T \approx 10^3 \div 10^4$ years), the star passes to the stage of a planetary nebula and therefore post-AGB stars are also commonly referred to as “protoplanetary nebulae” (PPNe). In the Hertzsprung–Russell diagram post-AGB stars move at almost constant luminosity leftward of the AGB and become increasingly hotter. These objects, which are descendants of AGB-stars, can be used to trace the physical and chemical parameters of the interstellar matter due to a change in the energy source, which is accompanied by a change of the star structure, ejection of the envelope, and mixing of matter.

The main task of our research is to reveal the chemical composition anomalies that are due to the nuclear synthesis of chemical elements in the interiors of low- and intermediate-mass stars (less than $8\text{--}9 M_{\odot}$) and subsequent dredge-up of the products of synthesis to the surface layers of stellar atmospheres. We use our high-precision spectroscopic data not only to study the chemical composition, but also to perform a detailed analysis of the velocity field in the atmospheres of these stars, which constitutes a separate astrophysical problem. In addition, the high quality observational data allowed us to produce an atlas of the spectrum of a typical post-AGB star over a wide wavelength interval. To this task, we chose the supergiant star HD 56126 ($Sp=F5Iab$), which is the optical component of the IR source IRAS 07134 + 1005 with a double-peaked spectral energy distribution (SED) typical of PPN. The star HD 56126 is located outside the galactic plane, its galactic coordinates are $l=206^{\circ}75$, $b=+9^{\circ}99$. Note that HD 56126 is a generally recognized **canonical object** in the phase of transition from the asymptotic giant branch to a planetary nebula. In addition to the anomalous SED mentioned above, which is due to the circumstellar dust, this star exhibits other, highly conspicuous, features specific for this class of objects [2]: the optical component of the PPN is an $F5Iab$ -type supergiant at a high galactic latitude; the central star is surrounded by an extended nebula, which, according to HST observations [3], has the largest angular size $\beta > 4''$ among PPN objects of this type; the optical spectrum exhibits variable complex emission–absorption profile of the $H\alpha$ and shows spectral features that are indicative of the current mass outflow. Based on their high-resolution spectroscopy ($R=860000$, $FWHM=0.35$ km/s) of HD 56126, Crawford and Barlow [4] revealed the multicomponent structure of the KI and C_2 features, which is indicative of repeated episodes of mass ejection from the star.

* The full version of the Atlas is available in electronic form from: <http://www.sao.ru/hq/ssl/Atlas/Atlas.html>

Subsequent studies of HD 56126 and of the associated IR source revealed a number of properties, which allowed the object to acquire the canonical status in its class. First, an analysis of the spectra obtained with the echelle spectrograph of the 6-m telescope, allowed Klochkova [5] to conclude that HD 56126 is a metal-poor star with $[Fe/H]_{\odot} = -1.0$ and high excess of carbon and *s*-process elements. Second, IRAS 07134+1005 was found to belong to the group of PPNe whose IR-spectra exhibit an emission feature at $\lambda = 21 \mu\text{m}$. Objects of this small subgroup were found to exhibit a correlation between the presence of this $21 \mu\text{m}$ -feature and the manifestation of products of stellar nucleosynthesis in the outer atmospheric layers: overabundance of carbon and heavy metals of the *s*-process. This so far unexplained correlation has been found independently by Klochkova [6] and a group of other authors [7]. Thus HD 56126 possesses the complete set of features peculiar to the entire family of PPNe, and this fact determines the importance of the detailed spectroscopy of this object and preparation of an atlas of its optical spectrum over a wide spectral region. This task is facilitated by HD 56126 being the brightest ($B=9^m11$, $V=8^m27$) star among carbon-rich PPNe and hence the most accessible star for high-resolution spectroscopy among the objects of this type.

Section 2 gives a brief description of the methods of observation and data reduction employed in this paper. Section 3 presents the peculiar features of the spectrum of HD 56126, and section 4 describes the field of radial velocities V_r in the atmosphere and envelope of the star. We also briefly discuss the radial-velocity variability and the variability of selected spectral-line profiles. Section 5 describes the spectroscopic atlas, identification of spectral features, and compares the spectrum of HD 56126 with that of the standard supergiant α Per ($Sp = F5Iab$).

2. Observations and reduction of spectra

We performed spectroscopic observations of HD 56126 and α Per with the 6-m telescope of the Special Astrophysical Observatory. We obtained all spectra with NES [8, 9] and Lynx [10, 11] echelle spectrographs operating in the Nasmyth focus. A 2048×2048 CCD and image slicer [12] with the NES spectrograph allows taking spectra with a resolution of $R \approx 60000$, whereas the Lynx spectrograph equipped with a $1K \times 1K$ CCD yields a resolution of $R \approx 25000$. The Table 1 gives the dates of observations and the spectral region recorded.

We use the modified ECHELLE context of MIDAS to extract data from two-dimensional echelle spectra (see [13] for details). Cosmic-hit removal was performed via median averaging of two successive spectra. Wavelength calibration was made using Th-Ar-lamps. We use DECH20 [14] code to perform spectrophotometric and position measurements. In particular, we determine the radial velocities from individual lines and their components by superimposing the direct and mirror-reflected profiles. We determine the position zero point for each spectrogram by referring it to the positions of ionospheric emission features of the night sky and to those of telluric absorptions, which show up against the spectrum of the object. The accuracy of **single line** velocity measurements in the spectra obtained is better than 1.0 and 1.5 km/s, for NES and Lynx spectrographs, respectively.

3. Peculiarities of the optical spectrum of HD 56126

Optical spectra of PPNe differ from the spectra of classical supergiants by the anomalous profiles of spectral lines (H α , NaI, HeI), and primarily, by the anomalous H α profiles. H α lines in the spectra of typical PPNe have complex emission and absorption profiles with asymmetric cores, P Cyg- or inverse P Cyg-type profiles, and profiles with two emission components. PPNe often exhibit a combination of several such features. Emission in H α may be due to mass outflow and/or pulsations and hence we must observe sporadic stellar wind in many PPNe. The Doppler shift of the core is usually smaller than the escape velocity, i.e., we have evidence only for motions at the wind base. The spectra of individual objects owe the great variety of their profiles to the differences in the dynamical processes in their extended atmospheres: spherically symmetric outflow with constant or height-dependent velocity, mass infall onto the photosphere, and pulsations. A two-component emission profile is indicative of a nonspherical envelope, e.g., the presence of a circumstellar disk.

The peculiarity of the optical spectra of PPNe often shows up not only in specific H α profiles, but also in the distortions of the spectral features of the *F* – *K*-type supergiant due to chemical composition anomalies and the presence of molecular features along with atomic and ion lines.

HD 56126 exhibits all these spectral peculiarities that distinguish PPN from a normal supergiant of the same spectral type. As is evident from Fig. 1, the H α line has a complex profile with absorption and emission components, which are absent in the spectrum of the comparison star α Per. Figure 1 also shows well-defined photospheric wings of the H α line in the spectrum of HD 56126. These wings are almost as extended as in the spectrum of α Per. Figure 2, which shows all the data now available, demonstrates date-to-date variations

Table 1. Log of observations and results of V_r measurements. Column 4 gives the mean V_r averaged over weak lines ($r \rightarrow 1$). For FeII(42), H α and D lines of NaI we give the velocities inferred from the positions of the strongest line components. The numbers in parentheses give the velocities inferred from weaker components. Slanted font in column 5 indicates the velocities inferred from the IR oxygen triplet OI λ 7773 Å. Semicolumn indicates uncertain data

Date	Spectrograph	$\Delta\lambda$, Å	V_r								
			$r \rightarrow 1$	FeII(42)	H β	H α	D NaI	C ₂	interstellar		
1	2	3	4	5	6	7	8	9	10	11	12
HD 56126											
12.01.93	Lynx	5560–8790	88.8	<i>91</i>	–	78 (100:)	77	–	–	–	–
10.03.93	Lynx	5560–8790	89.0	<i>93</i>	–	71 (43:)	75:	–	–	–	–
04.03.99	Lynx	5050–6640	85.9	77	–	76 (43:)	78	77.1	–	–	–
20.11.02	NES	4560–5995	89.6	95 (80:)	89	–	75 (89)	77.2	12.0	23.5	30.8
21.02.03	NES	5150–6660	88.8	96:	–	88 (112:)	75 (89)	77.1	12	24	31
12.04.03	NES	5270–6760	88.4	–	–	82 (103:)	75 (89:)	–	13	23	30.5
14.11.03	NES	4518–6000	85.3	96 (87:)	97	–	75 (87:)	76.9	12.5	–	–
10.01.04	NES	5270–6760	86.7	–	–	54:	76 (86:)	–	13.0	23.5	31
09.03.04	NES	5275–6767	89.8	–	–	58 (74:)	76 (89)	–	13	24	31
12.11.05	NES	4010–5460	82.5	97 (77:)	98	–	–	77.5	–	–	–
α Per											
04.03.99	Lynx	5050–6620	–1.2	–1	–	–2	–	–	–	–	–
02.08.01	NES	3500–5000	–1.8	–1 :	–2	–	–	–	–	–	–
11.11.05	NES	4010–5460	–2.0	–2	–2	–	–	–	–	–	–
12.11.05	NES	4560–6010	–1.9	–2	–2	–	–	–	–	–	–

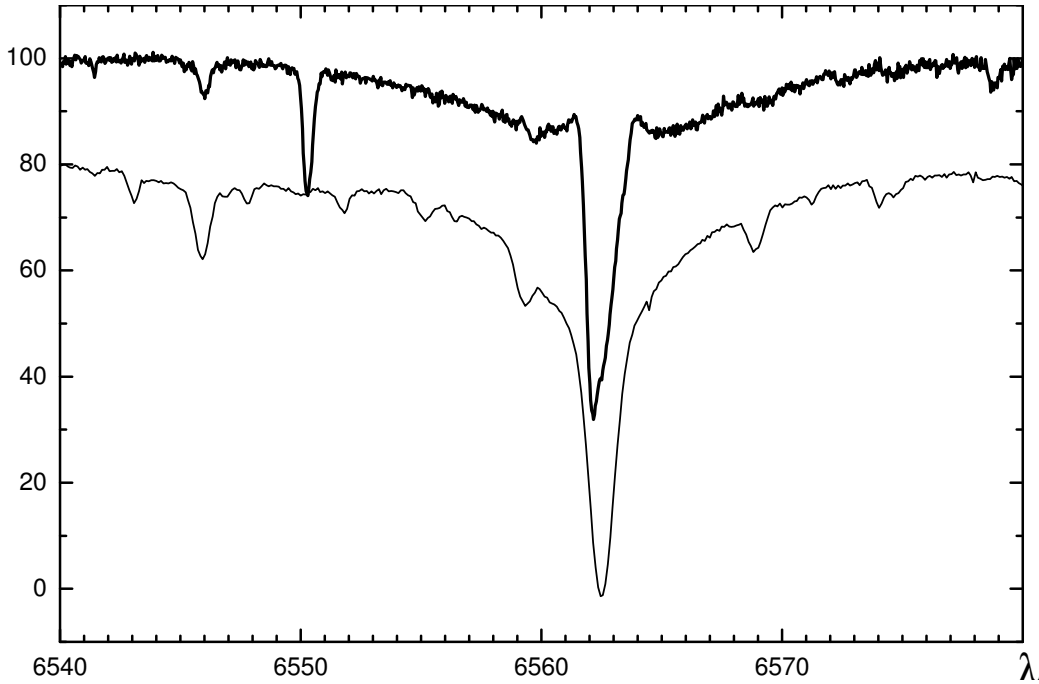


Figure 1. Fragment of the atlas containing the H α profile in the spectra of HD 56126 (top) and α Per (bottom). The y -axis gives the residual intensities, the continuum level is set equal to 100.

of the central part of the H α profile. Earlier, Oudmaijer and Bakker [15] performed spectral monitoring of HD 56126 and also found the H α to be highly variable over a two-months time scale. H α -line variability can be naturally explained in the case of post-AGB stars with signs of binarity (e.g., in the case of HR 4049 [16]), however, it also shows up in post-AGB objects, which exhibit no regular radial-velocity or light variations (the case of HD 133656 [17]). Photometric variability would allow us (like in the case of RV Tau type stars) to invoke the mechanism where a shock wave stimulates mass outflow. Based on an extensive set of good quality spectroscopic observations of HD 56126, Barthès et al. [18] found that not only the profile of H α but

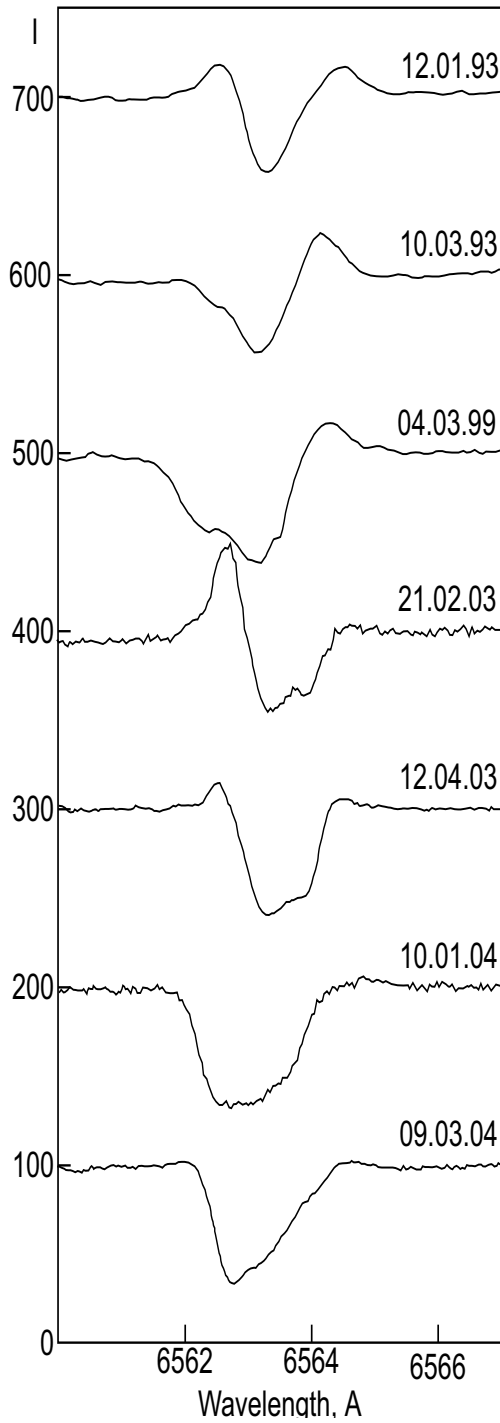


Figure 2. Variations of the $H\alpha$ -line profile in the spectra of HD 56126 taken on different days. The y -axis shows the residual intensities, the continuum level of the lower spectrum is set to 100 and every next spectrum is shifted by 100 gradations with respect to the previous spectrum.

also that of $H\beta$ to be variable. The above authors analyzed the variations of the profiles of both these lines and concluded that no periodic component is present that could be associated with the radial-velocity and photometric variations of the star.

The profiles of strong FeII lines (first and foremost, those of the members of the 42-nd multiplet), BaII, and other elements in the spectrum of HD 56126 are also variable. However, whereas either the blue or red wing may have lower slopes in the absorption core of $H\alpha$, nonhydrogen absorptions preserve their

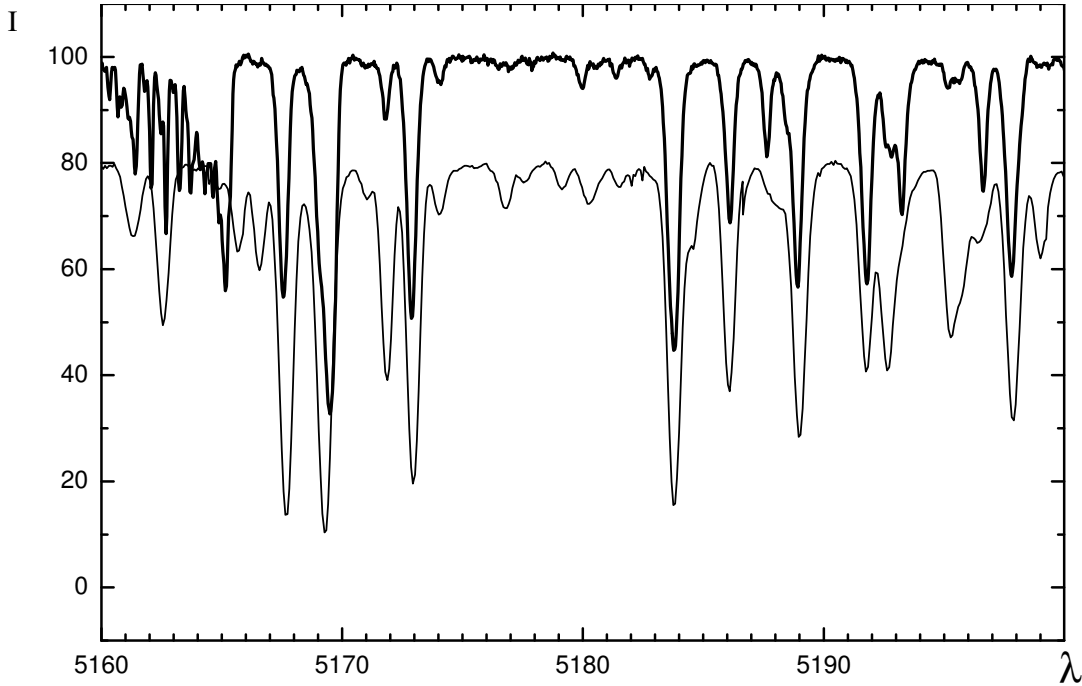


Figure 3. Same as Fig. 1, but for the spectral region containing the 5165 Å band of the Swan system of C₂ molecule and the FeII(42) 5169 Å line.

asymmetry pattern unchanged: the blue wing is always more extended than the red wing. The profile of the FeII (42) λ 5169 Å line in Fig.3 is a typical example.

Figures 3 and 4 show fragments of the spectra that may illustrate the differences between line intensities of HD 56126 and α Per. FeII absorptions in the spectrum of the former star are much weaker than in those of the latter star, and the ratio of the central depths of the same line in the spectra of the two stars depends on the line intensity: it increases from 1.5 to 4 as one passes from weak to strong lines. FeI lines are also depressed, on the average, by 0.1. On the contrary, CII absorptions as well as those of YII, ZrII, and other *s*-process products are deeper by 0.1–0.2 in the spectra of HD 56126 compared to the corresponding features in the spectrum of α Per.

Let us now analyze the molecular component of the spectrum of HD 56126. Bakker et al. [19] were the first to identify the Swan absorption bands of C₂ molecule and of the red system of CN molecule in the spectrum of the star. Later, Bakker et al. [20] used high-resolution spectra with $R=50000$ to perform a detailed analysis of molecular bands in the spectra of HD 56126 and 16 other PPNe selected based on the presence of carbon molecules C₂, CN, CH⁺ in their shells. Judging by the velocity corresponding to the position of these bands, the molecular spectrum forms in a limited region of the shell close to the star [20]. Our spectra exhibit several bands of the Swan system (see Fig. 3).

Here it is pertinent to recall that the spectra of several PPNe were found to exhibit emission Swan bands [19, 6]. However, the spectra of HD 56126 taken in different years show no signs of emission in these bands. D lines of NaI neither show any signs of emission. This fact is consistent with the rather simple elliptical shape of the nebula surrounding HD 56126. Emissions in the Swan bands or in NaI D lines appear to show up only in the spectra of PPNe with bright circumstellar nebulae with well-defined asymmetry. The spectroscopy of the following PPNe corroborates this hypothesis: IRAS 04296+3429 [21], IRAS 23304+6147 [22], AFGL 2688 [23], IRAS 08005–2356 [24], IRAS 20056+1834 [25], and IRAS 20508+2011 [26]. On HST images [3], the nebulae surrounding these PPNe are usually asymmetric and have a bipolar structure. Note also that most of the objects listed above belong to type “1” according to the classification of Trammell et al. [27] — i.e., they are PPNe with polarized optical radiation.

Figure 5 shows the behavior of the D2 NaI line profile in the spectrum of HD 56126, and here, like in Table 1, to reveal the fine structure of lines, we analyze only the spectra taken with the highest resolution. The positions of the three short-wavelength components remain constant within the errors. This stability confirms that the components form in the interstellar medium. The wavelength shift of the deepest component agrees

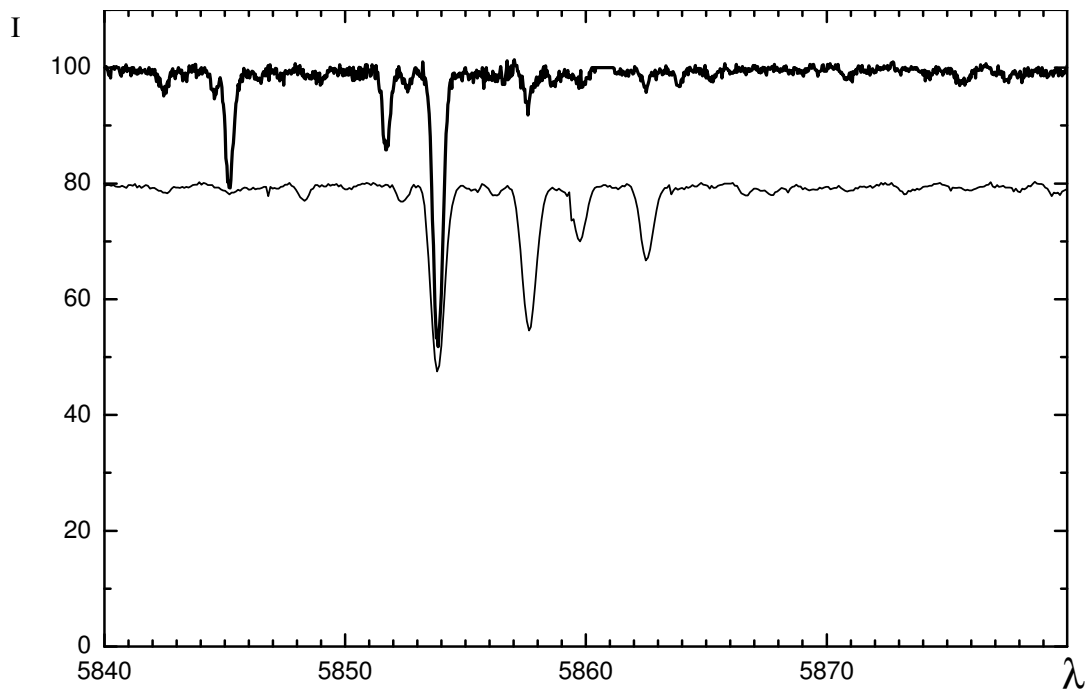


Figure 4. Same as Fig. 1, but for the spectral region with the BaII λ 5853 Å line.

with that of the Swan bands (columns 8 and 9 in Table 1), and this fact indicates that the component in question forms in the circumstellar shell. Finally, the longest-wavelength component forms in the photosphere: its temporal behavior agrees with that of other photospheric absorptions (columns 4 and 8 in Table 1).

4. Radial velocities pattern

Much attention has been paid to the radial-velocity variations of HD 56126 and to study the differences between the radial velocities inferred from lines of different types. Bujarrabal et al. [28] used CO millimeter-wave observations to find $V_r = 86.1$ km/s, which is natural to adopt as the systemic radial velocity of HD 56126. Based on an extensive collection of spectrograms with high temporal resolution and high S/N ratio, Oudmaijer and Bakker [15] analyzed the behavior of V_r and concluded that it is variable on a time scale of several months with a small amplitude ($V_r = 84 \div 87 \pm 2$ km/s). The above authors demonstrated the absence of variations on time scales ranging from several minutes to several hours. The variability of the radial velocity of HD 56126 also showed up when the radial-velocity measurements made with the 6-m telescope were compared to published data [5]. Lèbre et al. [29] performed a detailed spectroscopic monitoring of HD 56126. Fourier analysis of the available radial-velocity and photometric data led the above researchers to conclude that the dynamical state of the atmosphere of HD 56126 is similar to that of the atmospheres of RV Tau-type variables. The above authors interpreted the variability of $H\alpha$ in terms of shock propagation. Later, Lèbre et al. [30] analyzed the variability of two lines, $H\alpha$ and $H\beta$. They obtained additional spectroscopic data and determined the period of radial pulsations to be $P = 36.8$ days.

Barthès et al. [18] analyzed all the available reliable radial-velocity measurements made for HD 56126 (89 measurements over eight years) and concluded that radial velocity of this star varies with a half-amplitude of 2.7 km/s and the main period of $P = 36.8 \pm 0.2^d$. The period of photometric variability is the same and photometric amplitude is very small, $0^m.02$. However, the above authors found the variability pattern of the star to differ significantly from pulsations observed in RV Tau-type stars. Judging by its temperature [5], HD 56126 evolved further beyond the stage of RV Tau-type stars. The photometric and radial-velocity variations of HD 56126 may be due to first-overtone radial pulsations driven by shocks that generate complex asynchronous motions in the upper hydrogen layers of the star.

Table 1 presents the radial-velocity data we obtained for HD 56126. Given that a velocity gradient is very likely in the upper layers of the star's atmosphere, we report here the V_r values for individual lines and groups of lines. As is evident from Table 1, velocity variations inferred from weak absorptions (their residual

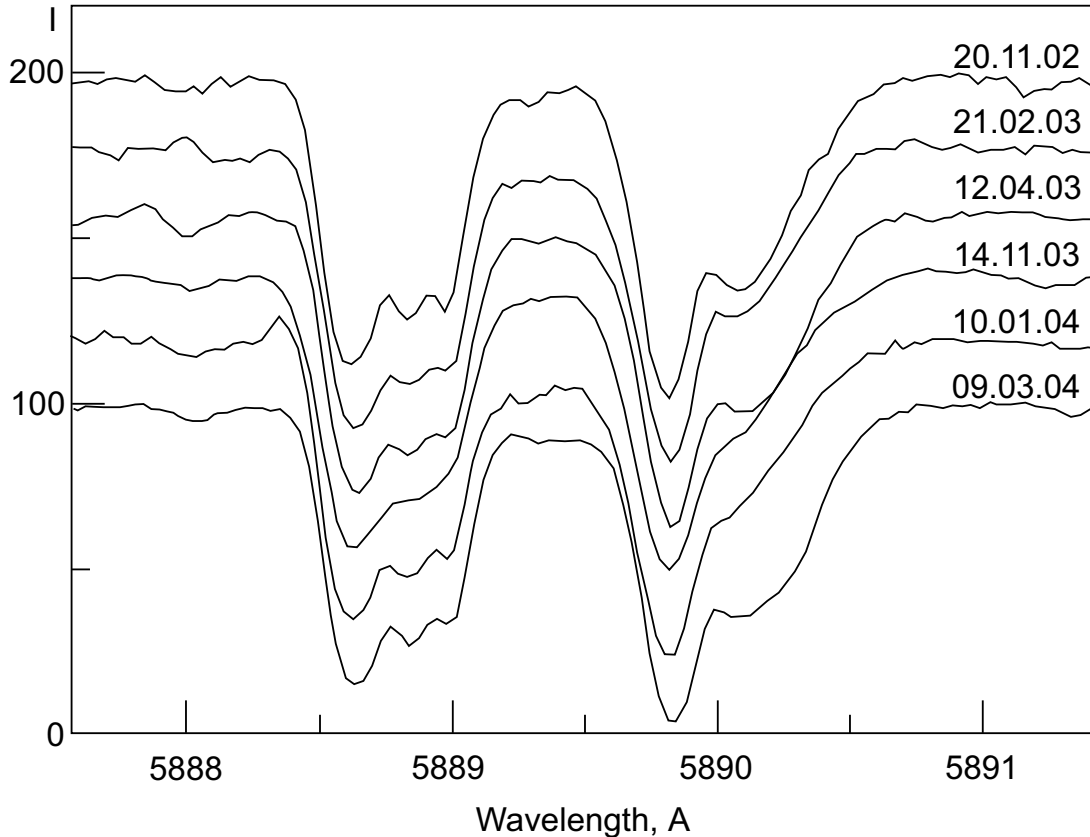


Figure 5. Spectral fragment with the D2 NaI line on different observing dates.

intensities approach 1) are within the variability limits established by Barthès et al. [18]. The positions of the circumstellar NaI D lines and Swan bands of the C_2 molecule agree well with each other and match the expansion velocity of the shell, $V_{exp} \approx 11$ km/s. Note that the position of the wind component of the $H\alpha$ line is inconsistent with those of the wind components of other lines, whereas the variations of the $H\beta$ profile is synchronized with those of FeII(42) lines.

When intercomparing our data and comparing it with those of other authors one must control the zero points of the corresponding radial-velocity systems. We used interstellar and circumstellar lines to control the radial-velocity zero points. Three blueshifted interstellar components of NaI lines in the spectrum of HD 56126, which are barely visible in Fig. 5, yield V_r values listed in Column 10–12 of Table 1. The fourth weak component with $V_r \approx 46$ km/s is barely visible in at least three our spectra. For each component, all our V_r estimates agree with each other and with those of Bakker et al. [19] within the quoted errors. Furthermore, as is evident from Fig. 5, the blend consisting of the three main components has sharp boundaries, which allow the velocity of this entire feature to be confidently measured. Its mean velocity as inferred from our data is equal to $V_r = 20.3 \pm 0.3$ km/s and agrees with the velocity of 20 ± 2 km/s measured by Lèbre et al. [29] from lower-resolution spectra. Crawford and Barlow [4] showed that when observed with superhigh resolution, the circumstellar C_2 and KI features exhibit components that are about 1 km/s apart. These components yield the same set of velocity values, but have different intensities. This effect may cause minor systematic differences (also on the order of 1 km/s) between the velocities inferred from circumstellar atomic and molecular lines in lower-resolution spectra. Our measurements reveal no variations of these velocities with time, and their mean values, 77.2 ± 0.5 and 75.4 ± 0.3 km/s for C_2 and NaI, respectively, do not disagree systematically with the radial velocities obtained by Lèbre et al. [29], Bakker et al. [19, 20], and Crawford and Barlow [4]: $77.3 \div 77.6$ and $75.3 \div 76.8$ km/s for C_2 and NaI, KI, respectively.

However, when comparing our V_r values with published data, one must take into account not only methodological effects, but also the spectroscopic peculiarity of the object itself. Line profiles in the spectrum of HD 56126 are asymmetric and their shape varies both with time and with line intensity. We plan to undertake a detailed analysis of the velocity field at different depths in the atmosphere and in the circumstellar envelope of HD 56126 in a separate paper.

As for the possible binarity of HD 56126, it has neither been confirmed or finally disproved. In this connection, of certain interest is a comment by Barthès et al. [18] who pointed out a weak trend in the star’s radial velocity over several years of observations. This trend maybe indicative of a second companion in the system with an orbital period longer than 16 years. Our eight spectra, which we took on more recent dates, fail to clarify the situation. It would be therefore important to follow the behavior of V_r over a several-years period taking one to two spectra every month on a regular basis.

The radial-velocity variability of HD 56126 is not a unique phenomenon. Part of candidate PPNe also demonstrate radial-velocity variations on a time scale of several hundred days, which may be indicative of the binary nature of these objects. Evidence for orbital motion has been obtained for several optically bright objects with IR excess. For example, authors of papers [31, 32] and [33] proved the binary nature, determined the orbital elements, and proposed models for the high-latitude supergiants 89 Her and HR 4049, respectively. Van Winckel et al. [34] showed that HR 4049, HD 44179, and HD 52961 to be spectral binaries with the orbital periods of about one to two years. The above authors concluded that all extremely metal-deficient PPNe studied so far (HR 4049, HD 44179, HD 52961, HD 46703, and BD +39°4926) are binary stars. The observed correlation between the binarity and the presence of a hot dust envelope indicates that binarity promotes the formation of an envelope. Bakker et al. [16] use high-resolution spectra of HR 4049 to analyze the variations of complex emission–absorption profiles of Na D lines and H α lines over the orbital period. Individual components of these lines may form under different conditions: in the atmosphere of the main star; in the disk where both components of the binary are immersed, or in the interstellar medium. For such binaries, of fundamental importance is the determination of the systemic velocity from radio spectroscopy.

The nature of the companions of suspected binary post-AGB stars remains unclear, because we see no direct manifestations of these companions either in the continuum or in spectral lines (all known binary post-AGB objects belong to type *SB1*). These companions may be either very hot object, or main-sequence stars of very low luminosity. For example, Bakker et al. [16] believe that the secondary companion in HR 4049 is a cold ($T_e = 3500$ K) MS star with a mass of $\mathcal{M}=0.56\mathcal{M}_\odot$, although it may also be a white dwarf, like in the case of Ba-stars [35].

Unfortunately, because of the short history of PPN studies we are so far unable to make any definitive conclusions concerning the cause of radial-velocity variability of a representative sample of these objects. Moreover, the observed pattern of radial-velocity variations is often complicated by differential motions in the extended atmospheres of these objects. A detailed analysis of radial velocities based on data taken with high spectral and temporal resolution for selected — the brightest — PPNe reveals differences in the behavior of radial velocities inferred from lines of different excitation, which form at different depths in the atmosphere of the star. For example, Bakker et al. [36] analyzed the spectrum of the IRAS source identified with the peculiar supergiant HD 101584 and found eight categories of spectral lines with fundamentally different temporal behavior of profiles, half-widths, and shifts (and hence of V_r values). In particular, the highest-excitation absorption features, which form near the star’s photosphere, exhibit radial-velocity variations due to the orbital motion in the binary system. At the same time, low-excitation lines with P Cyg-type profiles form in the stellar-wind region and are indicative of mass outflow. The systemic velocity has been confidently determined from radio emissions of CO and OH molecules.

5. Spectral atlas

Table 2. Spectra used to create this atlas

$\Delta\lambda$, Å	α Per		HD 56126	
	Date	Spectrograph	Date	Spectrograph
4010–5460	11.11.05	NES	12.11.05	NES
5460–6010	12.11.05	NES	9.03.04	NES
6010–6640	4.03.99	Lynx	9.03.04	NES
6640–8790			10.03.93	Lynx

Our comparative atlas of the spectra of HD 56126 and α Per includes 94 plots representing 40 Å-long spectral fragments. Some of them are shown in Figs. 1, 3, 4 and 6 to illustrate the differences between the

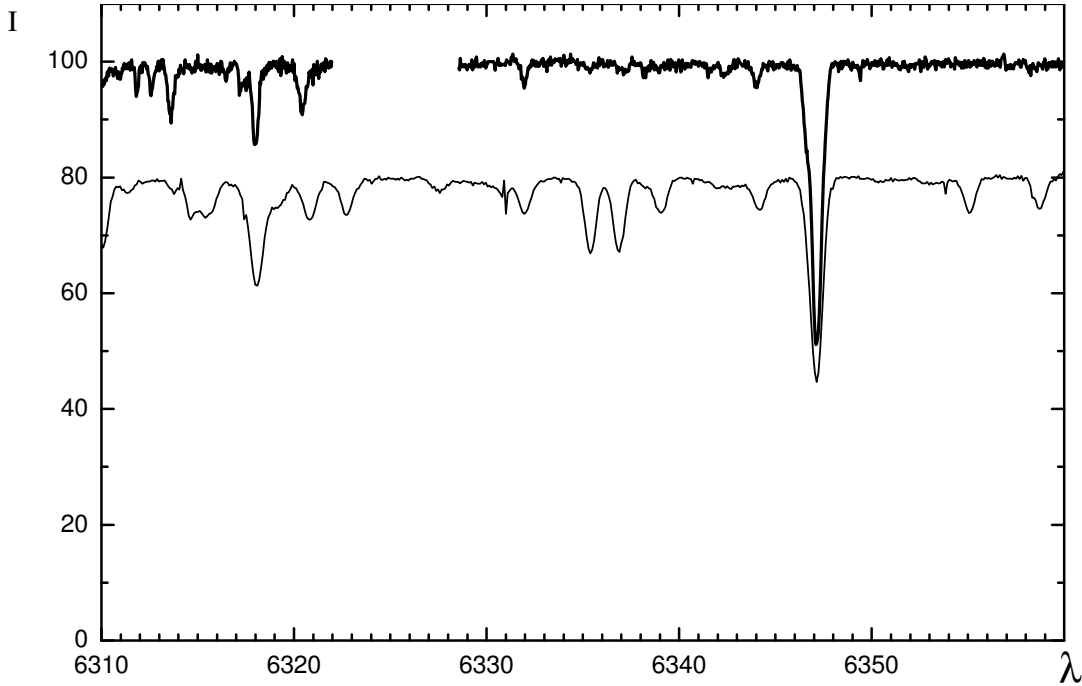


Figure 6. Same as Fig. 1, but for spectral fragment containing the SiII $\lambda 6347$ Å line.

intensities and profiles of lines in the spectra of two stars of similar temperature and luminosity. The full version of the atlas is available at <http://www.sao.ru/hq/ssl/Atlas/Atlas.html>.

In the wavelength interval 4010–6640 Å the atlas gives the complete spectra of both objects. However, in the more long-wavelength portion, up to 8790 Å, part of the spectrum has been lost in gaps between echelle orders and the remaining portions are overcrowded by telluric lines. The atlas therefore gives only the most informative fragments for this part of the spectrum of HD 56126.

The spectrum of HD 56126 is variable — line profiles, differential line shifts, and radial velocities vary from date to date, and therefore we performed no averaging of any kind — different spectral intervals are represented in the atlas by different spectra indicated in Table 2. For each wavelength interval, we selected from among the available spectra the one with the highest resolution and signal-to-noise ratio.

We supplement graphic data in the atlas with tables. In Table 3 column 1 gives the results of identification of spectral features; column 2, the laboratory wavelengths used to measure the radial velocities; columns 3 and 5, the central residual line intensities “ r ”, and columns 4 and 6, the heliocentric radial velocities V_r , measured from the line cores.

To identify atomic and molecular lines in the spectrum of HD 56126, we use the atlases and tables of solar spectrum [37, 38, 39, 40], the Moore tables for multiplets [41, 42], and electronic tables to the paper by Bakker et al. [19]. We also use VALD database [43]. We supplement the standard identification criteria (wavelength, relative line intensity, specific line profile) by two additional ones. One of these new criteria uses the chemical composition anomalies of HD 56126 mentioned above and the spectrum of the comparison star. The second new criterion can be applied only to sufficiently strong lines ($r < 0.5$), which in some of our spectra exhibit a sharp variation of radial velocity with line depth. Several rather strong lines remained unidentified in the spectrum of HD 56126. Some of them can be seen in the fragments of the atlas presented here: the $\lambda 6550$ Å line in Fig. 1, the $\lambda 5845$ and 5852 Å lines in Fig. 4, and the $\lambda 6347$ Å line in Fig. 6.

Compared to the lines in the spectrum of α Per, those in the spectrum of HD 56126 are less blended, because they are narrower and, in addition, many of these lines are weaker due to low metallicity of the star. However, by no means all absorptions can be used for reliable measurement of radial velocities. Table 3 lists about one and half thousand identifications for both stars and only 940 V_r measurements for HD 56126 obtained mostly from lines with minimal blending or from lines with the strongest difference of intensity in the spectra of two stars.

Conclusions

We use numerous high-resolution observations ($R=25000$ and 60000) made with the echelle spectrographs of the 6-m telescope to perform a detailed analysis of the optical spectrum of the post-AGB star HD 56126 identified with the IR source IRAS 07134+1005. We identified numerous absorptions of neutral atoms and ions in the wavelength interval from 4010 to 8790 Å and measured their depths and the corresponding radial velocities. We identified absorption bands of the C_2 , CN, and CH molecules, and interstellar bands (DIB). In addition to the known variability of the profile of the $H\alpha$ line, we found variations of the profiles of a number of FeII and BaII lines. We produced an atlas of the spectra of HD 56126 and its comparison star α Per.

An analysis of our radial velocities determined from all spectra of our collection leads us to conclude that:

- the accuracy of our radial-velocity data for HD 56126 allows them to be combined with the most accurate of earlier published measurements;
- we found the behavior of V_r values to differ for lines of different excitation degree, which form at different depth in the stellar atmosphere. The half-amplitude of the variations of radial velocities measured from weak absorptions ($r \rightarrow 1$) is equal to 2–3 km/s;
- we confirm the stability of the expansion velocity of the circumstellar envelope of HD 56126 as measured from C_2 and NaI lines;
- we reveal the complex and variable shape of the profiles of strong lines (not only hydrogen lines, but also absorption features of FeII, YII, BaII, and other elements), which form in the expanding atmosphere (wind base) of the star. To study the kinematic state of the atmosphere, one needs measurements of radial velocities for individual details of these profiles;
- we demonstrate the necessity of high and even superhigh spectral resolution for studying stellar and circumstellar lines, respectively, in the spectrum of HD 56126.

Acknowledgments

This work is supported by the Russian Foundation for Basic Research (project code 05–07–90087), the Presidium of the Russian Academy of Sciences (program “Origin and Evolution of Stars and Galaxies“, the Branch of Physical Sciences of the Russian Academy of Sciences (program “Extended Objects in the Universe”). This publication is based on work supported by Award No. RUP1–2687–NA–05 of the U.S. Civilian Research and Development Foundation (CRDF).

This work makes use of the SIMBAD, NASA ADS, and VALD astronomical databases.

References

1. T. Blöcker, *Astrophys. J.* **299**, 755 (1995).
2. S. Kwok, *Annu. Rev. Astron. & Astrophys.* **31**, 63 (1993).
3. T. Ueta, M. Meixner, and M. Bobrowsky, *Astrophys. J.* **528**, 861 (2000).
4. I.A. Crawford and M.J. Barlow, *MNRAS* **311**, 370 (2000).
5. V.G. Klochkova, *MNRAS* **272**, 710 (1995).
6. V.G. Klochkova, *Bull. Spec. Astrophys. Observ.* **44**, 5 (1998).
7. L. Decin, H. van Winckel, C. Waelkens, and E. Bakker, *Astron. & Astrophys.* **332**, 928 (1998).
8. V.E. Panchuk, V.G. Klochkova, I.D. Najdenov, Preprint of the Special Astrophysical Observatory of the Russian Academy of Sciences No. 135 (1999).
9. V.E. Panchuk, N.E. Piskunov, V.G. Klochkova, et al., Preprint of the Special Astrophysical Observatory of the Russian Academy of Sciences No. 169 (2002).
10. V.G. Klochkova, S.V. Ermakov, V.E. Panchuk, et al., Preprint of the Special Astrophysical Observatory of the Russian Academy of Sciences No. 137 (1999).
11. V.E. Panchuk, V.G. Klochkova, I.D. Najdenov, et al., Preprint of the Special Astrophysical Observatory of the Russian Academy of Sciences No. 139 (1999).
12. V.E. Panchuk, M.V. Yushkin, I.D. Najdenov, Preprint of the Special Astrophysical Observatory of the Russian Academy of Sciences No. 179 (2003).
13. M.V. Yushkin, V.G. Klochkova, Preprint of the Special Astrophysical Observatory of the Russian Academy of Sciences, No. 206 (2005).
14. G.A. Galazutdinov, Preprint of the Special Astrophysical Observatory of the Russian Academy of Sciences No. 192 (1992).
15. R. Oudmaijer and E.J. Bakker, *MNRAS* **271**, 615 (1994).
16. E.J. Bakker, D.L. Lambert, H. van Winckel, et al., *Astron. & Astrophys.* **336**, 263 (1998).
17. H. van Winckel, R. Oudmaijer, and N.R. Trams., *Astron. & Astrophys.* **312**, 553 (1996).
18. D. Barthès, A. Lèbre, D. Gillet, and N. Mauron, *Astron. & Astrophys.* **359**, 168 (2000).
19. E.J. Bakker, L.B.F.M. Waters, H.J.G.L.M. Lamers, et al., *Astron. & Astrophys.* **310**, 893 (1996).
20. E.J. Bakker, E.F. Dishoeck, L.B.F.M. Waters, and T. Schoenmaker, *Astron. & Astrophys.* **323**, 469 (1997).
21. V.G. Klochkova, R. Szczerba, V.E. Panchuk, and K. Volk, *Astron. & Astrophys.* **345**, 905 (1998).
22. V.G. Klochkova, R. Szczerba, V.E. Panchuk, *Astron. Lett.* **26**, 88 (2000).
23. V.G. Klochkova, R. Szczerba, V.E. Panchuk, *Astron. Lett.* **26**, 439 (2000).
24. V.G. Klochkova, E.L. Chentsov, *Astron. Rep.* **48**, 301 (2004).
25. N. Kameswara Rao, A. Goswami, and D.L. Lambert, *MNRAS* **334**, 129 (2002).
26. V.G. Klochkova, V.E. Panchuk, N.S. Tavganskaya, G. Zhao, *Astron. Rep.* **83**, 265 (2006).
27. S. Trammell, H.L. Dinerstein, and R.W. Goodrich, *Astrophys. J.* **108**, 984 (1994).
28. V. Bujarrabal, J. Alcolea, and P. Planesas, *Astron. & Astrophys.* **257**, 701 (1992).
29. A. Lèbre, N. Mauron, D. Gillet, and D. Barthes, *Astron. & Astrophys.* **310**, 923 (1996).
30. A. Lèbre, A. B. Fokin, D. Barthes, D. Gillet, and N. Mauron, *Astrophys. Space Sci.* **265**, 105 (2001).
31. A.A. Ferro, *PASP* **96**, 641 (1984).
32. L.B.F.M. Waters, C. Waelkens, M. Mayor, and N.R. Trams, *Astron. & Astrophys.* **269**, 242 (1993).
33. C. Waelkens, H.J.G.L.M. Lamers, L.B.F.M. Waters, et al., *Astron. & Astrophys.* **242**, 433 (1991).
34. H. van Winckel, C. Waelkens, and L.B.F.M. Waters, *Astron. & Astrophys.* **293**, L25 (1995).
35. R.D. McClure, *MNRAS* **96**, 117 (1984).
36. E. J. Bakker, H.J.G.L.M. Lamers, L.B.F.M. Waters, et al., *Astron. & Astrophys.* **307**, 869 (1996).
37. R.L. Kurucz, I. Furenlid, and J.T.L. Brault, *Nat. Solar Observ. Atlas*, New Mexico: National Solar Observatory (1984).
38. L. Wallace, K. Hinkle, and W. Livingston, *Nat. Solar Obs. Techn. Rep. No.00-001*, Tucson (2000).
39. A.K. Pierce and J.B. Breckinridge, *Contr. Kitt Peak Nat. Obs. No. 559* (1973).
40. J.W. Swensson, W.S. Benedict, L. Delbouille, and G. Roland, "The solar spectrum from λ 7498 to λ 12016. A table of measures and identifications", *Mem. Soc. Roy. Sci. Liege, Vol.hors ser. No.5* (1970).
41. C.E. Moore, *Contrib. Princeton University Observ. No.20, part I* (1945).
42. C.E. Moore, *Contrib. Princeton University Observ. No.20, part II* (1945).
43. N.E. Piskunov, F. Kupka, and T.A. Ryabchikova, *A&AS* **112**, 525 (1995).

Table 3. List of lines identified in the spectra of HD 56126 and α Per. Columns 3 and 5 list the central residual intensities of the lines (the continuum level is set to 1), and columns 4 and 6, the heliocentric velocities V_r .

Element	λ Å	α Per		HD 56126	
		r	V_r	r	V_r
TiII(11)	4012.39	0.13:	-2.2	0.05	81.7
FeI(557)	4013.64				
FeI(485)	4013.82	0.53:			
ScII(8)	4014.53	0.32:	-3.5	0.49	
CeII(157)	4014.90			0.56	
NiII(12)	4015.47	0.50:		0.64	84.8:
CeII(256)	4015.88			0.74:	83.0:
FeI(560)	4016.42	0.74:	-1.0		
FeI(279)	4017.10				
FeI(527)	4017.15	0.50:	-1.1	0.85:	
NiI(171)	4017.47	0.7:		0.9:	
MnI(5)	4018.10	0.47:			
FeI(560)	4018.27				
ZrII(54)	4018.38			0.53	82.5
NdII(19)	4018.83			0.89:	
VII(201)	4019.05	0.86:	-3.0:		
FeI(556)	4020.07				
NdII(19)	4020.87			0.80	82.4:
CoI(16)	4020.90	0.86:	-2.3		
NdII(36)	4021.33			0.79	82.0:
FeI(120)	4021.61				
FeI(278)	4021.87	0.45:	-3.9		
FeI(654)	4022.74				
NdII	4023.01			0.75:	81.2:
VII(32)	4023.38	0.47:	-2.5:	0.56	82.5
FeI(277)	4024.10				
ZrII(54)	4024.45			0.33:	85.1:
TiI(12)	4024.58	0.37:	-1.5:		
TiII(11)	4025.13	0.36:	-2.3	0.42:	83.5:
TiII(87)	4028.34	0.29:	-1.7	0.28:	84.8:
FeI(556)	4029.63	0.43:	-0.6:		
ZrII(41)	4029.68			0.28	83.4:
NdII(32)	4030.47			0.60:	
FeI(560)	4030.50				
MnI(2)	4030.76	0.18:		0.63	81.0:
CeII(108)	4031.34			0.52	
FeII(151)	4031.44				
LaII(40)	4031.68			0.42	84.6:
MnI	4031.78	0.46:	-2.0		
FeI(44)	4032.63	0.52:			
FeII(126)	4032.95			0.63	
MnI(2)	4033.06	0.26:	-3.3:		
ZrII(42)	4034.08			0.52:	83.7
MnI(2)	4034.48	0.39:	-2.6:		

Element	λ Å	α Per		HD 56126	
		r	V_r	r	V_r
ZrII(70)	4034.84			0.85:	83.1:
VII(32)	4035.60	0.35:		0.61	85.1
MnI(5)	4035.72				
VII(9)	4036.76	0.68:	-2.0	0.81	82.2:
GdII(49)	4037.39	0.90:		0.83	84.1:
CeII(218)	4037.67			0.81:	82.7:
GdII(49)	4037.90	0.85:		0.81:	
NdII(31)	4038.12			0.83:	
VII(32)	4039.56	0.82:	-2.0	0.89:	
FeI	4040.09	0.76:			
ZrII(54)	4040.24			0.58	83.5
FeI(655)	4040.64	0.52:			
CeII(138)	4040.76			0.52	82.6:
NdII(30)	4040.80				
MnI(5)	4041.35	0.48:	-2.5	0.84:	
CeII(140)	4042.58			0.60:	
SmII(4)	4042.72	0.59			
SmII(9)	4042.90			0.53	83.1:
FeI(276)	4043.90	0.56			
FeII(172)	4044.01			0.89	81.2:
FeI(359)	4044.61	0.60	-3.3:		
GdII(49)	4045.15			0.72:	
ZrII(30)	4045.63				
FeI(43)	4045.81	0.12	-4.6	0.22:	
FeI(557)	4046.06				
VII(177)	4046.27				
CeII(81)	4046.34			0.72	80.5
ZrII(43)	4048.68			0.29	84.2
MnI(5)	4048.75	0.39	-4.3		
ZrII(43)	4050.32	0.66		0.34	82.6:
VII(32)	4051.04				
NdII(66)	4051.15	0.69		0.75	
FeI(700)	4051.31				
CrII(19)	4051.97	0.54		0.64:	
TiII(87)	4053.82	0.33		0.39	83.2
FeI(698)	4054.82	0.51			
CeII(82)	4054.99			0.70	81.2:
MnI(5)	4055.54	0.68	-3.1		
TiII(11)	4056.19	0.60	-0.6	0.79	84.7
FeII(212)	4057.46			0.78	85:
MgI(16)	4057.50	0.48	-4.9		
CoI(16)	4058.22	0.75	-4.2:	0.89	
FeI(120)	4058.76	0.66		0.91	
MnI(5)	4058.92				
FeI(767)	4059.79	0.82	-3.3:		
NdII(63)	4059.96			0.88	
NdII(10)	4061.08	0.75	-2.4	0.66	81.0:
FeII(189)	4061.79	0.84:			
CeII(34)	4062.23			0.79	82.3

Element	$\lambda \text{ \AA}$	$\alpha \text{ Per}$		HD 56126	
		r	V_r	r	V_r
FeI(359)	4062.44	0.56	-1.0		
FeI(43)	4063.59	0.19	-4.0:	0.40	82.9
TiII(106)	4064.37	0.67	-1.5:	0.82	81.1:
VII(215)	4065.09	0.74		0.78	
FeI(698)	4065.38				
NiII(11)	4067.03	0.38		0.59	83.8
CeII(22)	4067.28			0.64	86:
FeI(559)	4067.98	0.54	-3.1	0.87	83.0
CeII(82)	4068.84			0.75	81.8
FeI(558)	4070.78	0.60			
ZrII(54)	4071.09			0.59	82.3:
FeI(43)	4071.74	0.23	-3.8	0.46	82.8
CrII(26)	4072.56	0.68	-3.1	0.77	85.5:
CeII(109)	4072.92			0.78	83.8:
CeII(4)	4073.48			0.61	83.4:
FeI(558)	4073.76	0.64			
GdII(44)	4073.76			0.70:	
FeI(524)	4074.79	0.61	-2.8	0.95:	
NdII(62)	4075.12			0.85:	
CeII(57)	4075.70				
SmII(51)	4075.85	0.53	-2.3:	0.51	
FeI(558)	4076.63				
LaII(11)	4076.71	0.37	-3.3:	0.74:	
ZrII(54)	4077.05			0.53:	
CrII(19)	4077.50				
SrII(1)	4077.71	0.09	-2.8	0.10	
DyII	4077.96				
CeII(19)	4078.32			0.67:	
FeI(217)	4078.35	0.56:	-0.7:		
MnI(5)	4079.3:	0.58		0.95:	
FeI(359)	4079.84	0.69	-2.1:		
FeI(558)	4080.21	0.74			
CeII(44)	4080.44			0.72	82.4:
CrII(165)	4081.21	0.80:		0.74	82.4:
CrII(165)	4082.29	0.77			
CeII(60)	4083.23			0.61	82.2
MnI(5)	4083.63	0.52	-1.8:		
FeI(698)	4084.49	0.62	-1.9:	0.88	
CeII(172)	4085.23	0.51		0.70	85.6
FeI(559)	4085.30				
VII(214)	4085.67			0.61	
ZrII(54)	4085.68			0.61	84.8:
CrII(26)	4086.13	0.70	-3.3:	0.85	84.0:
LaII(10)	4086.71	0.62	-2.1:	0.47	83.0
FeII(28)	4087.28	0.65		0.72	84.6:
FeII(39)	4088.75	0.74	-2.9:		
CrII(19)	4088.90			0.76	
ZrII(29)	4090.52	0.70	-3.7	0.43	82.4
CoI(29)	4092.39	0.62:			

Element	λ Å	α Per		HD 56126	
		r	V_r	r	V_r
HfII(6)	4093.16	0.84:	-3.2:	0.65:	82.5
CeII(160)	4093.96			0.83:	82.0:
CaI(25)	4094.93		-1.1:		
FeI(217)	4095.98				
ZrII(15)	4096.63			0.50	83.6
FeI(558)	4097.08		-3.2:		
H δ	4101.74	0.08	-2.0	0.06	96.0:
SiI(2)	4102.94		-2.9:		
DyII	4103.31				81.2:
FeI(356)	4104.12		-1.6:		
CeII(156)	4105.00			0.67:	
CeII(160)	4106.13			0.79:	
FeI(217)	4106.26	0.64:			
CeII(139)	4106.88			0.78:	
SmII(50)	4107.39			0.63:	85.1:
FeI(354)	4107.49	0.47	-3.4		
CaI(39)	4108.53	0.76:			
FeI(558)	4109.06	0.67:			
NdII(17)	4109.07			0.72:	83.3
NdII(10)	4109.46			0.61:	82.0
MgII(21)	4109.54				
FeI(357)	4109.80	0.51:			
ZrII(30)	4110.05			0.62:	82.4
CeII(29)	4110.39			0.74:	83.6:
CrII(18)	4110.99	0.52	-3.5	0.64	83.0:
CeII	4111.39			0.75:	
FeII(188)	4111.90	0.75:		0.86	82.3
FeI(695)	4112.32	0.80:			
CrII(18)	4112.55			0.91	82.5:
FeI(1103)	4112.96	0.62:			
CrII(18)	4113.22			0.86	83.6
CeII(137)	4113.73	0.86		0.80	81.8:
FeI(357)	4114.45	0.69	-2.7	0.95:	82.5:
KII(2)	4114.99				
CeII(22)	4115.37			0.79	81.6
CrII(181)	4116.66	0.86			
CeII(35)	4117.01			0.79	82.4:
CeII(77)	4117.29			0.83:	82:
FeI(700)	4117.85				
CeII(11)	4118.15	0.83:		0.69	81.7
FeI(801)	4118.54	0.38			
SmII(51)	4118.55			0.72	
CeII(89)	4119.01			0.83	80.7:
FeII(21)	4119.51	0.65:	-1.6	0.77:	
CeII(22)	4119.79			0.64	85:
FeI(423)	4120.21	0.72:			
CeII(112)	4120.83	0.87		0.71	81.0
CoI(28)	4121.32	0.67:	-1.6:	0.95:	
FeI(356)	4121.81	0.70:	-2.3	0.92	

Element	λ Å	α Per		HD 56126	
		r	V_r	r	V_r
FeII(28)	4122.66	0.37	-4.6	0.50	82.5
LaII(41)	4123.23	0.59		0.46	83.8:
FeI(217)	4123.75	0.62			
CeII(60)	4123.87			0.62	81.5
FeII(22)	4124.78				
YII(14)	4124.91	0.52		0.46	
FeI(1103)	4125.62				
FeI(354)	4125.88	0.71:		0.95:	
FeI(695)	4126.18	0.69:	-3.8:	0.97	85:
CeII(4)	4127.37			0.65	82.4
FeI(357)	4127.61				
FeI(558)	4127.80	0.42:		0.68:	
SiII(8)	4128.07	0.41:	-1.5:	0.50	84.2
FeII(27)	4128.74	0.49		0.63	82.7
CeII(227)	4129.18	0.61:		0.75	
EuII(1)	4129.72	0.60		0.85	81.1:
BaII(4)	4130.65			0.44	
CeII(209)	4130.71	0.56			
FeI(43)	4132.06	0.26	-1.5	0.58	83.4:
FeI(357)	4132.90	0.60	-4.5:		
CeII(4)	4133.80	0.61	-2.0	0.58	82.0
FeI(357)	4134.68	0.46		0.83	83.6
NdII	4135.33	0.83		0.73	
CeII(188)	4135.44				
FeI(726)	4137.00	0.61	-3.0		
CeII(2)	4137.65	0.67		0.57:	80.7:
FeII(150)	4138.21			0.78:	
FeII(39)	4138.40	0.70		0.73:	
FeI(18)	4139.93	0.82	-4.1		
FeI(695)	4140.41	0.86	-2.1		
LaII(40)	4141.73			0.72	81.2
HfII(87)	4141.84	0.77:			
CeII(10)	4142.40	0.68		0.69	81.8
VII(226)	4142.90			0.79	
FeI(523)	4143.42	0.41:		0.78	82.7
FeI(43)	4143.87	0.29	-2.7	0.59	82.1
CeII(3)	4144.49	0.86	-1.8:	0.76	83.6
CeII(9)	4145.00	0.80		0.70	81.7
CrII(162)	4145.76			0.82	
CeII(203)	4146.23			0.68	82.2
FeI(42)	4147.67	0.56	-3.7:	0.93	84.0:
ZrII(41)	4149.20	0.37		0.37	
FeI(694)	4149.36				
CeII	4149.94	0.72		0.61	81.0:
FeI(695)	4150.25	0.76			
ZrII(42)	4150.97	0.67	-3.2	0.43	82.8
CeII(2)	4151.97			0.55	82.1
FeI(18)	4152.17	0.45			
FeI(695)	4153.90	0.49	-0.2:	0.85	82.3

Element	λ Å	α Per		HD 56126	
		r	V_r	r	V_r
FeI(355)	4154.50	0.43		0.88	83.2
FeI(694)	4154.81			0.88	83.5
ZrII(29)	4156.25	0.43	-4.2:	0.38	80.9:
FeI(354)	4156.80	0.46			
FeI(695)	4157.78	0.58	-3.2		
FeI(695)	4158.80				
HfII(41)	4158.90	0.64			
CeII(246)	4159.03			0.80	80.6:
ZrII(42)	4161.21			0.35	84.2:
TiII(21)	4161.52	0.35		0.41	81.2:
SrII(3)	4161.80			0.49	
TiII(105)	4163.64	0.33	-2.4	0.38	82.6
CeII(10)	4165.59	0.72		0.64	83.7
BaII(4)	4166.00			0.75	82.0
MgI(15)	4167.27	0.53	-2.1	0.79	83.2
CeII(29)	4167.80	0.74		0.85	82.7
CeII(173)	4169.88	0.76		0.71	
FeI(482)	4170.91	0.52			
TiII(105)	4171.90			0.41	84.3
FeI(650)	4171.91	0.28			
FeI(689)	4172.64			0.85	81.8:
FeI(19)	4172.75	0.46			
FeII(27)	4173.46	0.22	-1.2	0.34	84.4
TiII(105)	4174.07	0.49	-2.2	0.74	84.2:
FeI(19)	4174.91	0.63	-2.9		
FeI(354)	4175.64	0.53	-2.0	0.78	83.2
FeI(689)	4176.57	0.60	-0.6	0.82	
FeI(18)	4177.59	0.22			
FeII(21)	4177.68			0.29:	83.0:
FeII(28)	4178.85	0.31	-1.5	0.38	84.5
CrII(26)	4179.43	0.49		0.60	83.9:
ZrII(99)	4179.81			0.49	82.4
FeI(354)	4181.75	0.38	-1.0:	0.78	83.4
FeI(476)	4182.39	0.71:	-2.1		
VII(37)	4183.45	0.60		0.82	81.1:
TiII(21)	4184.31	0.49		0.62	82.0:
FeI(355)	4184.89	0.59	-1.8	0.87	85.1:
CeII(124)	4185.33	0.93:		0.84	82.0
CeII(1)	4186.61			0.43	85.8:
FeI(152)	4187.04	0.41	-2.4	0.71	82.8:
FeII(152)	4187.80	0.36	-4.5	0.69	82.9
FeI(1116)	4188.73	0.68	-1.4	0.96	83.6
PrII(8)	4189.52			0.90:	83.1
FeI(940)	4189.56	0.84			
TiII(21)	4190.29	0.67	-2.4	0.89	82.3
VII(25)	4190.40				
CeII(169)	4190.63			0.87	80.8:
GdII(34)	4191.07				83.2:
FeI(152)	4191.43	0.38			

Element	λ Å	α Per		HD 56126	
		r	V_r	r	V_r
ZrII(108)	4191.50			0.57	
LaII(78)	4192.35			0.87:	
CeII(79)	4193.10	0.87		0.72	84.0:
CeII(85)	4193.87	0.89		0.84	81.5
FeI(693)	4195.33	0.50		0.87	83.7:
CrII(161)	4195.41				
FeI(693)	4196.21	0.58			
LaII(41)	4196.55			0.60:	
CeII(136)	4197.67			0.81	
CeII(209)	4198.00			0.79	
FeI(152)	4198.30	0.30		0.68	
CeII(207)	4198.43				
CeII(7)	4198.67			0.64	81.1:
FeI(522)	4199.09	0.40			
FeII(141)	4199.09				
NdII(15)	4199.10				
YII(5)	4199.27			0.60	
FeI(3)	4199.99	0.85			
FeI(689)	4200.93	0.73	-2.6:		
FeI(42)	4202.03	0.28		0.58	82.9
VII(25)	4202.34			0.80	82.6
CeII(186)	4202.94	0.78		0.71	82.6
LaII(53)	4204.03	0.52	-2.5:	0.80	81.9:
YII(1)	4204.75			0.50	80.8
VII(37)	4205.07	0.41	-3.0	0.65	
MnII(2)	4205.39	0.51		0.79:	
ZrII(133)	4205.91			0.84	81.1
HfII(74)	4206.59			0.85	83.7:
FeI(3)	4206.70	0.67	-1.2		
MnII(2)	4207.23	0.66	-3.2:		
CrII(26)	4207.35			0.92	83.1
FeI(689)	4208.61	0.66:			
ZrII(41)	4208.98	0.56	-2.3		
CrII(162)	4209.02			0.42	82.6:
CeII(3)	4209.41				
VII(25)	4209.74	0.73		0.88	83.5:
FeI(152)	4210.35	0.47	-1.0		
ZrII(97)	4210.62			0.64	82.3
ZrII(15)	4211.89	0.57	-2.6	0.39	83.5
CeII(169)	4213.04			0.88	
FeI(355)	4213.65	0.71	-2.5	0.95:	
CeII(203)	4214.03			0.84	82.5
FeI(274)	4215.43				
SrII(1)	4215.52	0.15	-0.6	0.16	96.9
FeI(3)	4216.18	0.51	-2.9		
CdII(49)	4217.20			0.88	82.5:
FeI(693)	4217.55	0.61	-2.6	0.75	83.3
FeI(800)	4219.36	0.51	-2.1	0.85	83.7
CaII(16)	4220.13			0.88:	

Element	λ Å	α Per		HD 56126	
		r	V_r	r	V_r
NdII(32)	4220.26	0.68			
FeI(482)	4220.35				
FeII(152)	4222.21	0.48			
ZrII(80)	4222.41				
CeII(36)	4222.60			0.52:	
FeI(689)	4224.17				
ZrII(29)	4224.28	0.50:		0.66	81.0
FeI(689)	4224.52				
CrII(162)	4224.85			0.83	83.6
VII(37)	4225.22				
PrII(8)	4225.33			0.73:	
FeI(693)	4225.45	0.44			
FeI(521)	4225.95	0.74:			
CaI(2)	4226.72	0.21	-3.6	0.43	80.7:
FeI(693)	4227.43	0.32	-4.7	0.59:	
NdII(19)	4227.72			0.73:	82.6
NdII(36)	4228.20				
Cl	4228.32	0.86		0.77	81.9
SmII(4)	4229.70	0.76		0.92:	
FeI(41)	4229.76				
LaII(83)	4230.95			0.92	83.2:
NiI(136)	4231.03	0.91			
ZrII(99)	4231.64			0.52	83.5
HfII(72)	4232.43	0.86:		0.78	82.2
FeII(27)	4233.17	0.23		0.34	86.5
FeI(152)	4233.60	0.40:			
NdII(20)	4234.20			0.83	81.9
VII(24)	4234.22	0.83			
MnI(23)	4235.14				
MnI(23)	4235.29	0.73			
VII(5)	4235.74			0.46	
FeI(152)	4235.94	0.31			
ZrII(110)	4236.54	0.84:		0.64	83.0
LaII(41)	4238.38			0.63	82.3
FeI(693)	4238.81	0.52	-2.6	0.79	81.6
FeI(18)	4239.85	0.51	-3.8	0.67	
CeII(2)	4239.91				
FeI(764)	4240.38				
CaI(38)	4240.45	0.77			
CrII(31)	4242.37	0.47	-1.2	0.53	83.3
NiII(9)	4244.80	0.84		0.88	81.0:
FeI(352)	4245.26	0.61		0.94	
FeI(691)	4245.35				
HfII(72)	4245.84			0.72	
CeII(158)	4245.98				
FeI(906)	4246.09	0.69			
ScII(7)	4246.83	0.25	-2.1	0.39	88.7:
NdII(14)	4246.88				
FeI(693)	4247.42	0.47	-2.7		

Element	λ Å	α Per		HD 56126	
		r	V_r	r	V_r
FeI(482)	4248.23	0.72			
CeII(1)	4248.68	0.82	-2.8:	0.69	81.8
FeI(152)	4250.12	0.41	-1.7	0.69	82.6
FeI(42)	4250.79	0.33	-2.2	0.58	81.8
GdII(15)	4251.74	0.84		0.80	82.1
CrII(31)	4252.63	0.64	-3.0	0.74	82.4
CeII(77)	4253.36			0.81	82.5
CrI(1)	4254.34	0.35	-1.3	0.68	82.8
CeII(81)	4255.78			0.76	83.0
CeII(172)	4256.16			0.83:	
NdII(59)	4256.24	0.81	-3.1	0.84:	
CeII(123)	4257.12			0.92	81.0:
ZrII(15)	4258.05				
FeII(28)	4258.15	0.34	-0.5	0.36	
FeI(3)	4258.32				
FeI(476)	4260.13				
FeI(152)	4260.47	0.31	-1.5	0.57	83.2
CeII(19)	4261.16			0.95	81.2
CrII(31)	4261.92	0.49	-2.2	0.55	83.5
SmII(37)	4262.68			0.94	81.5:
CeII(254)	4263.43			0.78	
FeI(692)	4264.21	0.84	-2.3		
CeII(239)	4264.37			0.91	81.2
FeI(993)	4264.74	0.90			
YII(71)	4264.88			0.78	
ZrII(98)	4264.92				
FeI(993)	4265.26	0.87			
MnI(23)	4265.92	0.91	-2.5		
ZrII(8)	4266.72			0.86	82.9
FeI(273)	4266.97	0.78	-3.8		
FeI(482)	4267.83	0.73	-1.9	0.93	84:
CrII(192)	4268.93	0.75:			
Cl(16)	4269.02			0.68	
CrII(31)	4269.29	0.65		0.69:	
CeII(204)	4270.19	0.90	-2.8	0.77	81.5
CeII(21)	4270.72			0.82	81.0:
FeI(152)	4271.16	0.40	-2.7	0.70	82.0
FeI(42)	4271.76	0.25	-1.3	0.44	82.8
FeII(27)	4273.32	0.44		0.43:	
ZrII(28)	4273.52				
FeI(478)	4273.88	0.90:			
CrI(1)	4274.79	0.37	-2.1	0.72	82.7
CrII(31)	4275.56	0.54	-1.7	0.57	83.6
FeI(597)	4276.68	0.87			
ZrII(40)	4277.37	0.84		0.70	82.4
FeII(32)	4278.16	0.59	-1.6	0.71	82.8
VII(225)	4278.89	0.90		0.83	82.4:
SmII(27)	4279.68			0.92	82.7:
FeI(351)	4279.87	0.82			

Element	λ Å	α Per		HD 56126	
		r	V_r	r	V_r
CeII(225)	4280.14			0.88	82.2:
GdII(15)	4280.48	0.82		0.89	82.4
SmII(46)	4280.79			0.84:	
SmII	4281.01				
CrII(17)	4281.03	0.79			
MnI(23)	4281.10				
ZrII(182)	4282.21			0.58	
FeI(71)	4282.40	0.41	-1.7		
CaI(5)	4283.01	0.58	-2.3	0.92	81.7
CrII(31)	4284.20	0.60	-1.2	0.69	83.1
MnII(6)	4284.43			0.82:	83.0:
NdII(10)	4284.51				
CeII(11)	4285.37			0.82	82.8
FeI(597)	4285.44	0.71	-2.3		
TiI(44)	4286.01	0.84			
FeI(414)	4286.47	0.84	-1.9		
ZrII(69)	4286.51			0.63	82.6
LaII(75)	4286.97	0.76	-3.3	0.75	81.7
TiII(20)	4287.88	0.36	0.1	0.51	82.9
CeII(135)	4289.45			0.79	82.0:
CrI(1)	4289.72	0.33:			
TiII(41)	4290.21	0.24	-2.0:	0.36	85.0:
TiI(44)	4290.94	0.79	-3.5:		
FeI(3)	4291.46	0.76	-1.4		
MnII(6)	4292.25	0.82			
CeII(205)	4292.77			0.88	83.0:
ZrII(110)	4293.14	0.91		0.63	82.0
TiII(20)	4294.10	0.28	-2.2	0.37	83.9
FeI(41)	4294.12				
ScII(15)	4294.78	0.55	-2.3	0.73	82.5
LaII(53)	4296.05	0.73		0.65	83.1:
FeII(28)	4296.57	0.35	-0.4	0.37	
CeII(2)	4296.68				
PrII(7)	4297.76			0.92	84.3:
FeII(520)	4298.04	0.78			
FeI(152)	4299.23	0.31		0.60	
CeII(47)	4299.36				
TiII(41)	4300.05	0.24	-0.7	0.31	93.0:
TiI(44)	4301.09	0.74:			
ZrII(109)	4301.81				
TiII(41)	4301.92	0.31	-0.8	0.40	81.5
CaI(5)	4302.53	0.46	-3.0:	0.79	83.2
FeII(27)	4303.17	0.34	-1.7	0.41	84.2:
NdII(10)	4303.59				
FeI(414)	4304.55	0.86	-3.4		
FeI(476)	4305.45			0.49	83.5:
ScII(15)	4305.71	0.37			
CeII(1)	4306.72	0.81		0.75	82.3
CaI(5)	4307.75				

Element	λ Å	α Per		HD 56126	
		r	V_r	r	V_r
TiII(41)	4307.89	0.21	-3.7:	0.40	82.4
FeI(42)	4307.90				
ZrII(88)	4308.94			0.70	82.4
FeI(849)	4309.03	0.72:			
YII(5)	4309.63	0.38		0.40	84.8:
CeII(126)	4309.74				
CeII(133)	4310.70			0.91	82.1
ZrII(99)	4312.23			0.84	82.9
TiII(41)	4312.86	0.33	-2.3	0.41	83.5
ScII(15)	4314.09	0.22		0.36:	
FeII(32)	4314.30				
TiII(41)	4314.98	0.25	-1.1	0.43	83.8
GdII(43)	4316.05	0.97:		0.95	82.0:
TiII(94)	4316.80	0.58	-1.6	0.69	82.7
ZrII(40)	4317.32	0.82:		0.56	81.9
CaI(5)	4318.65	0.56	-0.1	0.90	83.4:
ScII(15)	4320.74	0.22		0.38	
TiII(41)	4320.95				
FeI	4321.79	0.87	-1.9		
LaII(25)	4322.50	0.88	-0.9	0.75	82.7
ZrII(141)	4323.62			0.91	81.0
FeI(70)	4325.00				
ScII(15)	4325.01	0.33	-2.6	0.46	81.9:
FeI(42)	4325.76	0.25	-2.4	0.43	81.4:
BaII(7)	4326.74	0.73		0.90	
MnII(6)	4326.76				
FeI(761)	4327.10				
GdII(15)	4327.13	0.75		0.92	82.5
FeI(597)	4327.91	0.83	-1.6	0.89	83.0
SmII(15)	4329.03	0.89	-2.8	0.92	
TiII(94)	4330.24	0.51		0.64	
CeII(82)	4330.45				
TiII(41)	4330.70	0.44	-3.5	0.59	81.8:
NiI(52)	4331.65	0.77	-2.7		
VII(23)	4331.79			0.87	
ZrII(132)	4333.28			0.59:	82.1
LaII(24)	4333.76	0.59	-0.7	0.53:	82.4
LaII(77)	4334.96			0.80:	81.7:
CaII(89)	4336.26			0.69:	
FeI(41)	4337.05	0.36:			
TiII(94)	4337.33				
CeII(82)	4337.78			0.38:	
TiII(20)	4337.92	0.23:	-3.7:	0.33	
NdII(68)	4338.70	0.49:		0.52	82.5:
H γ	4340.47	0.09	-2.1	0.08	97.0:
TiII(32)	4341.36	0.30:			
FeI(645)	4343.26	0.61:			
TiII(20)	4344.29	0.30:		0.47:	82.1
CeII(251)	4345.96			0.80:	

Element	λ Å	α Per		HD 56126	
		r	V_r	r	V_r
FeI(598)	4346.56	0.74:			
FeI(828)	4347.84	0.78			
FeI(414)	4348.94	0.85:	-1.8:		
CeII(59)	4349.79	0.85		0.78	81.2
VII(36)	4349.97				
TiII(94)	4350.84	0.52		0.71	83.2
FeII(27)	4351.77	0.23	-1.1	0.36:	85.6:
MgI(14)	4351.91				
FeI(71)	4352.73	0.53	-2.5		
CeII(220)	4352.73			0.76	
FeII(213)	4354.36				
LaII(58)	4354.40			0.70	83.3:
ScII(14)	4354.61	0.58	-5.7:		
CaI(37)	4355.19	0.81	-3.3:		
FeII	4357.57			0.90	83.8:
NdII(10)	4358.17			0.80	81.6
NdII(57)	4358.70				
YII(5)	4358.72	0.58	-5.6	0.48	83.7
NiI(86)	4359.63				
GdII(67)	4359.64	0.57			
ZrII(79)	4359.74			0.43	82.8
FeII	4361.25	0.93	-1.7	0.92:	
CeII(157)	4361.66			0.92:	
SmII(45)	4362.04				
NiII(9)	4362.09	0.80	-2.0	0.86	82.5
LaII(133)	4363.05	0.93	-1.9	0.95:	
MoII(3)	4363.64			0.92:	81.5:
GdII(33)	4364.14			0.91:	81.9:
YII(70)	4364.17	0.96			
CeII(135)	4364.66	0.88	-1.9	0.74	81.4
LaII(53)	4344.66				
FeI(415)	4365.90	0.92			
FeI(414)	4367.58				
TiII(104)	4367.66	0.41	-0.6:	0.56	82.6
FeI(41)	4367.91				
CeII(227)	4368.23	0.82:		0.79	83.0:
FeII	4368.26				
NdII(11)	4368.63	0.93:		0.91:	82.3:
FeII(28)	4369.40	0.53		0.67	83.1
FeI(518)	4369.77	0.66:		0.90:	
ZrII(79)	4370.96	0.73:		0.48	81.9
Cl(14)	4371.37	0.69:		0.70	83.2:
FeII(33)	4372.22	0.92		0.92	
FeI(214)	4373.57	0.83			
CeII(202)	4373.82			0.83	81.5:
ScII(14)	4374.46	0.30		0.43	
TiII(93)	4374.82	0.28		0.44:	81.6:
YII(13)	4374.94			0.29:	94.7:
NdII(8)	4375.04				

Element	$\lambda \text{ \AA}$	$\alpha \text{ Per}$		HD 56126	
		r	V_r	r	V_r
FeI(2)	4375.93	0.49	-2.1	0.78	81.1
FeI(471)	4376.78	0.91	-1.5		
MoII(3)	4377.77	0.94:	-3.1:	0.92	82.3:
LaII(77)	4378.10			0.93	
VI(22)	4379.23	0.82	-1.2:		
ZrII(88)	4379.78	0.70	-3.3		
CeII(155)	4380.06			0.43	83.0
CdII(68)	4380.64	0.91		0.98:	
CeII(2)	4382.17	0.87	-2.9	0.73:	81.2:
FeI(799)	4382.78	0.82	-1.7:		
ZrII(97)	4383.10			0.85:	
FeI(41)	4383.54	0.25	-2.2	0.40	82.6
FeII(32)	4384.32	0.50		0.61	83.9
ScII(14)	4384.81	0.46		0.74	
FeII(27)	4385.38	0.36	-2.2	0.44	84.0
NdII(50)	4385.66				
CeII(57)	4386.84				
TiII(104)	4386.85	0.51		0.57	81.0:
FeI(476)	4387.90	0.79			
CeII(5)	4388.01			0.87	81.0:
FeI(830)	4388.41	0.72	-2.2		
ZrII(140)	4388.50			0.90	80.0:
FeI(2)	4389.25	0.90	-3.1		
VI(22)	4389.99	0.87	-2.0:		
MgII(10)	4390.56			0.76	
FeI(414)	4390.96				
TiII(61)	4391.02	0.48		0.67	82.2
CeII(81)	4391.66	0.76		0.66	82.1
TiII(51)	4394.04	0.44	-2.6	0.54	83.2
TiII(19)	4395.03	0.25	-1.5	0.36	87.7
TiII(61)	4395.84	0.48	-2.5	0.58	83.0
YII(5)	4398.02	0.49		0.44	84.1
TiII(61)	4398.29				
CeII(81)	4398.79			0.89	80.4:
CeII(81)	4399.20			0.75	82.4
TiII(51)	4399.77	0.34	-2.3	0.44	83.1
ScII(14)	4400.40	0.36		0.50	83.3
NdII(10)	4400.83			0.80	
FeII(828)	4401.29	0.55			
ZrII(68)	4401.35			0.84	83.6:
ZrII(79)	4403.35	0.76		0.60	81.9
FeI(41)	4404.75	0.28	-1.6	0.49	82.5
VI(22)	4406.65	0.90	-3.3		
GdII(103)	4406.67			0.94	81.9:
CeII(64)	4407.28			0.90	81.1:
FeI(68)	4407.70	0.56	-2.6	0.79	81.5
FeI(68)	4408.42	0.58	-2.2	0.92	83.0:
PrII(4)	4408.84			0.85	82.0
TiII(61)	4409.24	0.50		0.77:	

Element	$\lambda \text{ \AA}$	$\alpha \text{ Per}$		HD 56126	
		r	V_r	r	V_r
TiII(61)	4409.52			0.75:	
NiI(88)	4410.52				
CeII(33)	4410.64			0.79:	
TiII(115)	4411.08	0.58	-2.8	0.62	82.3
TiII(61)	4411.93	0.64	-1.1	0.78	84.2:
NdII(9)	4412.27			0.93	
FeII(32)	4413.59	0.69	0.3:	0.79	84.5:
PrII(26)	4413.77				
ZrII(79)	4414.54	0.82:		0.55	82.5
FeI(41)	4415.12	0.29	-0.7:	0.57	83.4
ScII(14)	4415.56	0.38:		0.54	82.3
FeII(27)	4416.82	0.38	-2.0	0.43	83.4
TiII(40)	4417.72	0.34	-2.2	0.41	82.9
TiII(51)	4418.34	0.48	-2.1	0.59	82.2
CeII(2)	4418.78	0.85:		0.70	81.6
SmII(32)	4420.53			0.87	
ScII(14)	4420.67	0.79			
SmII(37)	4421.13	0.94		0.88	82.3
TiII(93)	4421.94	0.58	-1.9	0.68	82.9
FeI(350)	4422.57	0.55	-1.4		
YII(5)	4422.59			0.46	82.7
FeI(412)	4423.14	0.76			
TiII(61)	4423.22			0.92	82.9
CeII(21)	4423.68			0.89	81.2
FeI(830)	4423.84	0.88			
SmII(45)	4424.34	0.82	-4.2:	0.83	81.4
CaI(4)	4425.44	0.62	-1.5	0.93	81.3
FeI(2)	4427.31	0.46		0.87:	81.7:
TiII(61)	4427.90	0.82	-2.2:	0.79	82.5
CeII(19)	4429.27	0.86	-3.1	0.73	83.0
LaII(38)	4429.92	0.68		0.60	81.3
FeI(68)	4430.62	0.63	-2.9	0.95	81.3:
ScII(14)	4431.37	0.75	-2.7	0.92	81.3
TiII(51)	4432.10	0.79		0.94	83.6
LaII(11)	4432.95			0.94	
FeI(830)	4433.22	0.77	-2.0		
GdII(82)	4433.64			0.93	
SmII(41)	4433.89	0.76		0.84	84.5:
SmII(36)	4434.32			0.86	80.7
CaI(4)	4434.96	0.49	0.0	0.89	82.2
FeI(2)	4435.15				
EuII(4)	4435.58			0.89	83.9:
CaI(4)	4435.68	0.57			
GdII(117)	4436.23	0.89		0.95	
FeI(516)	4436.93	0.88	-1.4		
CeII(169)	4437.61	0.95:	-1.0:	0.93	81.7
GdII(67)	4438.13			0.97:	
GdII(44)	4438.27				
FeI(828)	4438.35	0.91	-2.7		

Element	λ Å	α Per		HD 56126	
		r	V_r	r	V_r
FeII(32)	4439.16	0.95	-3.8	0.95	83.0:
FeI	4439.89	0.95			
ZrII(79)	4440.45	0.81	-1.3:	0.57	83.4
CeII(238)	4440.88	0.89		0.89:	
TiII(40)	4441.73	0.55	-2.0	0.69	82.8
FeI(68)	4442.34	0.52	-0.9		
ZrII(53)	4442.50			0.72	80.8:
ZrII(88)	4443.00	0.53		0.43	83.1
FeI(350)	4443.20				
TiII(19)	4443.80	0.29	-1.5	0.42	86.8
LaII(133)	4443.94				
TiII(31)	4444.56	0.46	-2.9	0.56	83.3
ZrII(96)	4445.88			0.87	84.8
NdII(49)	4446.39	0.86	-2.3:	0.84	80.3
FeI(68)	4447.72	0.56	-1.6	0.89	83.1
CeII(202)	4449.33	0.81		0.74	82.4
FeII(222)	4449.66	0.88		0.85	82.0:
TiII(19)	4450.48	0.34	-1.4	0.47	84.7
FeII	4451.55			0.73	82.9
MnI(22)	4451.59	0.71	-2.9:		
NdII(6)	4451.98			0.93:	
SmII(26)	4452.73	0.91		0.91	81.0:
TiI(113)	4453.32	0.87			
VII(199)	4453.35				
FeII(350)	4454.39				
SmII(49)	4454.63				
CaI(4)	4454.78	0.41	-1.5	0.52	84.4
FeII	4455.26			0.89	
LaII(53)	4455.79			0.87	
CaI(4)	4455.89	0.63	-3.2		
NdII(50)	4456.39			0.90	82.9
CaI(4)	4456.62	0.78		0.91	83.8:
ZrII(79)	4457.42			0.62	82.4
TiI(113)	4457.44	0.75			
FeI(992)	4458.08				
MnI(28)	4458.25	0.78			
SmII(7)	4458.52			0.93	81.4
FeI(68)	4459.12	0.46	-1.8	0.85	82.1
CeII(2)	4460.21	0.77	-0.7	0.67	82.0
ZrII(67)	4461.22			0.52	82.9:
FeI(2)	4461.65	0.43			
FeI(471)	4462.00				
NdII(54)	4462.41	0.85			
NdII(50)	4462.98	0.88		0.82	82.1
CeII(20)	4463.41			0.83	81.2
TiII(40)	4464.45	0.39		0.52	83.4:
MnI(22)	4464.68				
HfII(72)	4466.41				
Cl	4466.48			0.76	84.3

Element	λ Å	α Per		HD 56126	
		r	V_r	r	V_r
FeI(350)	4466.55	0.52	-2.1		
SmII(53)	4467.34	0.88	1.2	0.82	
TiII(31)	4468.49	0.29	-1.8	0.41	86.9
TiII(18)	4469.16			0.73	82.7
FeI(830)	4469.37	0.46			
TiII(40)	4470.85	0.50	-1.7	0.62	84.0:
CeII(8)	4471.24			0.68	81.6:
FeI(595)	4472.72				
FeII(37)	4472.92	0.52		0.64	82.9
FeII(17)	4474.19	0.96		0.98	81.0:
VII(199)	4475.70			0.98:	
FeI(350)	4476.02	0.52	-1.1	0.88	84.0
YI(14)	4477.46	0.91	-1.8		
Cl	4477.47			0.85	82.5
Cl	4478.59				
SmII	4478.66	0.85	-1.2	0.81:	81.5
GdII(15)	4478.80				
Cl	4478.83			0.85:	
CeII(203)	4479.36			0.77	81.7:
CeII(124)	4479.43				
FeI(828)	4479.61	0.80:			
FeI(515)	4480.14	0.82			
MgII(4)	4481.22	0.28	-2.2	0.26	82.5
ZrII(131)	4482.04				
FeI(2)	4482.17	0.48		0.86:	
FeI(68)	4482.26				
TiI(113)	4482.74	0.85	-2.0:		
GdII(62)	4483.33	0.97		0.93	84.4
CeII(3)	4483.90			0.79	81.7
FeI(828)	4484.23	0.73			
	4484.80			0.92	
ZrII(79)	4485.44			0.83	84.4
FeI(830)	4485.68	0.81	-3.6		
HfII(23)	4486.14			0.97	83.4
CeII(57)	4486.91	0.85	-1.0	0.74	81.7
TiII(115)	4488.33	0.52	-3.9	0.60	82.7
FeII(37)	4489.17	0.42	-2.7	0.53	83.2
FeI(2)	4489.74	0.73:			
FeI(973)	4490.77	0.83	-3.0:	0.97	
FeII(37)	4491.40	0.42	-1.5	0.51	83.2
TiII(18)	4493.52	0.67	-1.5	0.81	81.7
ZrII(130)	4494.41			0.54	84.0:
FeI(68)	4494.56	0.47	-3.6		
CeII(154)	4495.39				
ZrII(79)	4495.44	0.82		0.76	82.7
TiII(40)	4495.46				
FeII(147)	4495.52				
TiI(146)	4496.15	0.88			
TiI(8)	4496.25			0.90	82.5:

Element	λ Å	α Per		HD 56126	
		r	V_r	r	V_r
CrI(10)	4496.86				
ZrII(40)	4496.96	0.56		0.45	84.3
CeII(19)	4497.84	0.90		0.89	82.9
MnI(22)	4498.90	0.88			
CrI(150)	4500.28				
TiII(18)	4500.32	0.77		0.88	
TiII(31)	4501.27	0.30	-2.1	0.44	86.0
MnI(22)	4502.22	0.90:	-1.6:		
CrII(16)	4504.52				
FeI(555)	4504.83	0.93			
NdII(7)	4506.58			0.93	
TiII(30)	4506.74	0.83	-2.5		
GdII(13)	4506.93				
CrII(16)	4507.19				
FeII(38)	4508.28	0.37	-2.3	0.46	83.8
CrII(191)	4511.82	0.90	-0.8		
TiI(42)	4512.74	0.90	-1.7	0.95	
FeII(37)	4515.35	0.37	-2.3	0.46	83.6
LaII	4516.38			0.92:	
CrII(191)	4516.56	0.94			
FeI(472)	4517.53	0.88	-1.7		
TiI(42)	4518.03				
TiII(18)	4518.30	0.60	-1.3:	0.77	
VII(212)	4518.38				
SmII(49)	4519.63	0.93:		0.87	80.5
FeII(37)	4520.22	0.38	-2.5	0.46	83.3
GdII(44)	4521.30	0.97:			
FeII(38)	4522.63	0.30	-2.8	0.41	84.1:
TiI(42)	4522.80				
CeII(2)	4523.08				
BaII(3)	4524.94			0.72	81.5
LaII(50)	4526.12			0.82	80.8
FeI(969)	4526.45	0.73	-1.1		
CeII(108)	4527.35	0.79:	-2.0:	0.72	82.3
VII(56)	4528.50			0.61	
FeI(68)	4528.61	0.36	-2.8		
TiII(82)	4529.48	0.46	-0.1:	0.63	83.3
FeI(39)	4531.15	0.57		0.95	81.4
TiI(42)	4533.24			0.91	81.6:
TiII(50)	4533.96	0.23		0.34	
FeII(37)	4534.16				
TiI(42)	4534.78	0.78	-1.9	0.95	
SmII(45)	4537.95	0.94		0.92	
CrII(39)	4539.62	0.69			
CeII(108)	4539.77			0.66	
FeII(38)	4541.52	0.46	-2.9	0.55	82.5
TiII(60)	4544.02	0.64	-2.9	0.79	81.8
TiII(30)	4545.14	0.57	-2.4	0.74	81.3:
CrI(10)	4545.96	0.83	-2.8		

Element	λ Å	α Per		HD 56126	
		r	V_r	r	V_r
FeI(755)	4547.85	0.79	-1.9	0.97	
FeII(38)	4549.47				
TiII(82)	4549.62	0.15		0.28	90.5:
CeII(229)	4551.30	0.93:		0.86	80.0:
TiII(30)	4552.30	0.61:		0.86	82.2
BaII(1)	4554.03	0.29	-2.1	0.31	88.7
CrII(44)	4554.99	0.58	-2.2	0.64	83.0
FeII(37)	4555.89	0.33		0.45	84.0
CrII(44)	4558.65	0.38	-2.6	0.45	82.1
CeII(8)	4560.28			0.78	82.2
CeII(2)	4560.96	0.90	-1.8:	0.83	82.2
CeII(1)	4562.36	0.81	-2.0	0.69	81.9
TiII(50)	4563.76	0.32	-2.2	0.41	84.7
ZrII(116)	4565.41			0.82	84.2:
CrII(39)	4565.77	0.60:		0.71	83.0
TiII(60)	4568.32	0.73	-1.1	0.88	82.6
HfII(86)	4570.70			0.89	80.3:
MgI(1)	4571.10	0.82	-1.1		
TiII(82)	4571.98	0.27	-1.5	0.36	91.3:
ZrII(139)	4574.48			0.69	84.6:
LaII(23)	4574.87	0.83:		0.78	80.6:
FeII(38)	4576.34	0.47	-2.1	0.54	83.0
FeII(26)	4580.06	0.59		0.70	82.7
CeII(7)	4582.50			0.75:	
FeII(37)	4582.83	0.51	-2.2	0.58	82.6
TiII(39)	4583.41				
FeII(38)	4583.84	0.28	-2.3	0.41	87.5
CrII(44)	4588.20	0.45	-2.0	0.49	83.1
CrII(44)	4589.94	0.43	-1.8	0.53	83.4
CrII(44)	4592.05	0.58	-1.7:	0.65	82.8
CeII(6)	4593.92	0.74:		0.72	81.1
FeI(820)	4596.06			0.87	80.1:
NdII(51)	4597.01			0.93	82.9
VII(56)	4600.19	0.67		0.90	82.8
FeII(43)	4601.36	0.84:	-2.8	0.91	83.6
ZrII(138)	4601.97	0.86:	-0.4:	0.89	82.6
FeI(39)	4602.94	0.63	-2.2	0.94	81.8
CeII(6)	4606.40	0.87:		0.83	82.1
TiII(39)	4609.27	0.85	-2.8	0.94	82.5
FeI(826)	4611.28	0.73	-2.4		
ZrII(67)	4613.95	0.87	-1.2:	0.69	82.6
CrII(44)	4616.62	0.61	-2.0	0.68	83.3
CrII(44)	4618.82	0.49	-2.2	0.55	82.3
LaII(76)	4619.87			0.85	82.3
FeII(38)	4620.51	0.55	-1.7	0.63	83.4
CeII(27)	4624.90			0.77	83.7:
FeI(554)	4625.05	0.76			
CeII(1)	4628.16	0.83	-1.9	0.67	82.6
ZrII(139)	4629.07				

Element	λ Å	α Per		HD 56126	
		r	V_r	r	V_r
FeII(37)	4629.33	0.38	-2.7	0.44	82.7:
CrII(34)	4634.07	0.54	-2.1	0.59	83.0
FeII(186)	4635.31	0.79	-1.6	0.79	82.9
TiII(38)	4636.33	0.81	-2.4	0.91	82.9
FeI(822)	4638.02	0.80:		0.95	82.1
SmII(36)	4642.24	0.96	-2.7	0.93	82.5
LaII(8)	4645.28	0.95:		0.93	80.9:
CrI(21)	4646.17	0.71	-1.4	0.95	
FeI(409)	4647.44	0.72	-2.6	0.91	80.8:
FeII(25)	4648.93			0.91	82.4:
CrI(21)	4651.29	0.86	-1.7		
CrI(21)	4652.16	0.78	-1.7		
CeII(154)	4654.29			0.77	83.4:
LaII(75)	4655.49			0.82	82.0
FeII(43)	4656.98	0.43		0.64	
TiII(59)	4657.20				
ZrII(129)	4661.78			0.74	82.3:
LaII(8)	4662.51			0.80	82.3:
FeII(44)	4663.71	0.69	-1.6	0.77	83.4
FeII(37)	4666.75	0.51	-2.0	0.61	83.1
LaII(76)	4668.91			0.91	82.1
FeII(25)	4670.19				
ScII(24)	4670.40	0.43		0.60	82.1:
LaII(80)	4671.82			0.92	82.7:
CeII(18)	4680.13			0.92	81.6
YII(12)	4682.34	0.73		0.61	81.4
CeII(228)	4684.61			0.89	81.1:
ZrII(129)	4685.19	0.86		0.73	82.7
LaII(23)	4691.17			0.95	82.4:
FeI(409)	4691.42	0.75	-1.2:		
LaII(75)	4692.50			0.91	81.4
TiII(59)	4698.67			0.93	81.9
MgI(11)	4702.99	0.52	-2.2		
ZrII(138)	4703.03			0.63	81.9
NdII(3)	4706.55	0.92	-1.1:	0.89	82.2
TiII(49)	4708.66	0.59		0.76	82.5
C ₂ (1;0)R1(16)	4712.96			0.92:	
C ₂ (1;0)R2(15)	4713.12			0.92:	77.2:
C ₂ (1;0)R1(15)	4714.38			0.91	77.6
C ₂ (1;0)R2(14)	4714.54			0.91:	78.0:
C ₂ (1;0)R3(13)	4714.72			0.93:	77.7
NdII(49)	4715.60			0.91:	
C ₂ (1;0)R3(12)	4716.15			0.96	78.4:
LaII(52)	4716.44			0.92	82.2:
C ₂ (1;0)R1(13)	4717.08			0.93	77.4
C ₂ (1;0)R2(12)	4717.29			0.94	78.1
C ₂ (1;0)R3(11)	4717.48				78.0
C ₂ (1;0)R1(12)	4718.38			0.92	78.2
C ₂ (1;0)R2(11)	4718.60			0.93	77.4

Element	λ Å	α Per		HD 56126	
		r	V_r	r	V_r
C ₂ (1;0)R3(10)	4718.84			0.95	77.8
C ₂ (1;0)R1(11)	4719.61			0.87:	78.3:
C ₂ (1;0)R1(10)	4720.81			0.93	77.7
C ₂ (1;0)R2(09)	4721.09			0.94	78.7
C ₂ (1;0)R3(08)	4721.36			0.95	77.4
C ₂ (1;0)R1(09)	4721.94			0.95	78.3
C ₂ (1;0)R2(08)	4722.27			0.91	78.8:
C ₂ (1;0)R3(07)	4722.53			0.94	77.8
C ₂ (1;0)R1(08)	4723.04			0.93	78.0
C ₂ (1;0)R2(07)	4723.44			0.90	77.2
C ₂ (1;0)R3(06)	4723.74			0.94	77.6
C ₂ (1;0)R1(07)	4724.08			0.93	77.7
C ₂ (1;0)R3(05)	4724.83			0.92	77.9
C ₂ (1;0)R1(06)	4725.07			0.88:	78.3:
C ₂ (1;0)R2(05)	4725.57			0.91	79.6
C ₂ (1;0)R1(05)	4725.99			0.86:	78.5:
C ₂ (1;0)R2(04)	4726.60			0.89	77.5
C ₂ (1;0)R1(02)	4728.47			0.77	77.9:
C ₂ (1;0)P1(34)	4730.77			0.90	78.0
FeII(43)	4731.47	0.51	-3.1	0.59	81.3
C ₂ (1;0)P2(03)	4732.81			0.89	78.3:
C ₂ (1;0)P2(04)	4733.40			0.84	78.6:
C ₂ (1;0)P2(05)	4733.93			0.83	
FeI(554)	4736.77	0.63	-0.3	0.73	84.0:
LaII(8)	4740.27	0.84		0.78	81.9
LaII(75)	4743.08	0.92		0.85	82.7
PrII(3)	4744.93			0.95	82.2
CeII	4747.14	0.97		0.92	82.4
LaII(65)	4748.73	0.93	-0.9:	0.83	81.5
FeI(634)	4757.58	0.91	-0.8		
CeII	4757.84			0.94	81.4
MnI(21)	4761.53	0.85	-2.5:		
ZrII(107)	4761.67			0.63	82.1
Cl(6)	4762.31				
Cl(6)	4762.54			0.63:	
TiII	4763.90	0.58	-2.4	0.75	81.8:
TiII(48)	4764.53	0.64	-0.5:	0.83	
MnI(21)	4766.43	0.76			
Cl(6)	4766.68			0.83	82.2
Cl(6)	4770.03	0.88	-3.6	0.76	82.3
Cl(6)	4771.75			0.54	81.9
CeII(17)	4773.94	0.93	-3.9	0.90	80.6
Cl(6)	4775.91	0.84	-2.2	0.71	82.0
TiII(92)	4779.99	0.52	-2.7	0.60	82.3
MnI(16)	4783.42	0.70	-2.0	0.96	82.4
YII(22)	4786.58			0.59	82.5
TiII(17)	4798.53	0.64	-3.0	0.81	82.8
LaII(37)	4804.04	0.96	-1.1:	0.91	82.0
TiII(92)	4805.09	0.45	-1.5	0.53	83.2

Element	λ Å	α Per		HD 56126	
		r	V_r	r	V_r
LaII(37)	4809.00			0.89	82.4
NdII(3)	4811.35	0.93		0.91	82.0
CrII(30)	4812.35	0.73	-2.6	0.81	82.5
CrI(5)	4812.92			0.95	83.0:
ZrII(66)	4816.47	0.97		0.87	82.5
CrI(5)	4817.37	0.95:	-1.5:	0.90	81.7
NdII(47)	4820.34			0.91	81.9
YII(22)	4823.31			0.53	82.6
MnI(16)	4823.51				
CrII(30)	4824.14	0.47	-2.9	0.54	82.0
NdII(3)	4825.48	0.82:		0.86	82.0
CrI(5)	4826.80	0.95	-2.1	0.91	82.7:
NiI(111)	4831.18	0.83	-1.9	0.95	81.4
FeII(30)	4833.19	0.85	-1.8	0.94	82.9
CrII(30)	4836.23	0.67		0.78	82.2
LaII(37)	4840.02			0.92	81.4:
ZrII(138)	4841.98			0.92	82.6
SmII(26)	4844.21			0.95	82.2:
CeII(17)	4846.57			0.96	81.1:
CrII(30)	4848.25	0.52	-2.0	0.59	82.9
YII(22)	4854.87		-2.1:		83.0
FeI(318)	4859.74			0.80	
H β	4861.33	0.11	-1.7	0.13	98.2
CrII(30)	4864.32		-1.7:		83.3:
TiII(29)	4865.62		-2.6:		81.7:
FeI(318)	4871.32	0.50:	-2.6:	0.75	81.2
FeI(318)	4872.14	0.55:	-3.1:	0.83	81.9
TiII(114)	4874.01	0.65:	-2.2:	0.70	82.5
CrII(30)	4876.40			0.61	
CrII(30)	4876.48	0.51			
CaI(35)	4878.14				
FeI(318)	4878.22	0.56		0.90	81.0:
YII(12)	4881.44			0.92	81.1
CeII	4882.46			0.85	81.3
YII(22)	4883.69	0.51	-2.8	0.39	84.8
CrII(30)	4884.60	0.75	-0.9:	0.84	83.2
FeI(318)	4890.76	0.53	-2.2	0.78	80.8
FeI(318)	4891.49	0.49	-2.2	0.74	82.7
FeII(36)	4893.82	0.79	-1.6	0.86	
ZrII(107)	4894.43			0.89	82.0
BaII(3)	4899.94				
YII(22)	4900.12	0.46		0.38	
FeI(318)	4903.31	0.66	-1.9	0.87	81.0
ZrII(145)	4908.67			0.97	80.8:
TiII(114)	4911.19	0.59	-1.1:	0.63	83.7:
ZrII(3)	4911.66			0.82	81.8:
FeI(318)	4918.99	0.52	-2.8	0.81	82.9
FeI(318)	4920.50	0.42	-1.1	0.64	85.0:
LaII(7)	4920.98			0.63	81.9:

Element	λ Å	α Per		HD 56126	
		r	V_r	r	V_r
LaII(7)	4921.80	0.79		0.67	82.3
FeII(42)	4923.92	0.29	-1.8	0.55:	78.0:
				0.39	93.9
Cl(13)	4932.05	0.81	-3.4	0.64	81.3
BaII(1)	4934.08	0.32	-2.9	0.35	85.5
FeI(687)	4946.39	0.79	-1.9		
LaII(36)	4946.47			0.92	80.8
FeII(168)	4953.98	0.93	-1.6:	0.94	83.3:
FeI(318)	4957.30				
FeI(318)	4957.60	0.31		0.65	81.8:
NdII(1)	4959.13	0.92	-1.1	0.92	81.4
NdII(22)	4961.40	0.96		0.93	82.4
SrI(4)	4962.29			0.78	83.3
FeI(687)	4966.09	0.71	-2.3	0.94	83.2
OI(14)	4967.88			0.95	
FeI(1067)	4967.90	0.83	-1.9		
OI(14)	4968.79			0.96:	82.1:
LaII(37)	4970.39			0.85	81.7
CeII	4971.48			0.88	82.2
FeI(984)	4973.11	0.82	-2.0		
TiII(71)	4981.35			0.94	80.8
TiII(38)	4981.74	0.72	-1.2		
YII(20)	4982.13			0.69	82.4
LaII(22)	4986.82	0.93		0.86	82.8
NdII	4989.96	0.95	-2.0:	0.90	81.4:
FeII(36)	4993.35	0.65	-1.1:	0.75	82.9
FeI(16)	4994.14	0.73	-2.4:	0.93	82.0:
LaII(37)	4999.46			0.78	82.6
TiI(38)	4999.49	0.75	-2.1		
TiII(71)	5005.17	0.78:		0.92	82.2
FeI(984)	5005.72				
FeI(318)	5006.12	0.54:		0.88	82.1
TiII(113)	5010.21	0.77	-2.9	0.87	82.8
BaII(10)	5013.00			0.92	80.1
TiII(71)	5013.69	0.64	-2.7	0.81	82.0
Cl	5017.09			0.91:	82.8:
FeII(42)	5018.44	0.28	-2.2	0.55:	77.0:
				0.34	96.4
CaII(15)	5019.98	0.72	-3.0:	0.82	82.8:
TiI(38)	5020.03				
FeI(965)	5022.24	0.74:			
CeII(16)	5022.87			0.90	81.3:
Cl	5023.85	0.94:		0.87	82.7
TiI(38)	5024.85	0.90:			
Cl	5024.92			0.94	81.8
ScII(23)	5031.02	0.53	-2.6	0.63	82.5
Cl(4)	5039.07			0.76	82.3
Cl	5040.13			0.90	82.4:
SiII(5)	5041.03			0.77	80.5:

Element	λ Å	α Per		HD 56126	
		r	V_r	r	V_r
CeII(16)	5044.01			0.89	81.9
FeI(318)	5044.22	0.86			
FeI(114)	5049.82	0.64	-2.1	0.93	81.8
FeI(16)	5051.64	0.62	-0.9:		
Cl(12)	5052.17	0.74:		0.54	81.7
Cl	5053.52			0.95	83.6
SiII(5)	5055.98	0.83	-1.1:	0.75	83.3:
SiII(5)	5056.31				
FeI(1094)	5065.02	0.66	-1.7:	0.93:	81.3:
FeI(383)	5068.77	0.68		0.95:	
TiII(113)	5069.09			0.93	83.0:
FeI(1089)	5272.08				
TiII(113)	5072.29	0.63		0.79	82.4
FeI(1094)	5074.75	0.71	-1.7	0.94	81.6
CeII(15)	5079.68			0.80	81.6
FeI(16)	5079.75	0.74			
NiII(143)	5080.54	0.74	-2.1	0.94	81.4
FeI(16)	5083.35	0.72	-2.1	0.97	
YII(20)	5087.42	0.62	-2.4	0.51	84.3
FeI(1090)	5090.78	0.82	-2.0	0.94	82.9:
NdII(48)	5092.80	0.94	-1.2	0.92	82.0
C ₂ (0;0)R1(33)	5095.15			0.98	77.5:
C ₂ (0;0)R1(32)	5098.13			0.98	77.3:
C ₂ (0;0)R3(30)	5098.30			0.98:	78.3:
FeII	5100.74	0.70		0.81	82.3:
C ₂ (0;0)R1(29)	5106.36			0.95	77.5
FeI(16)	5107.45				
LaII(164)	5107.54	0.57		0.90	83.0:
FeI(36)	5107.65				
FeI(1)	5110.42	0.68	-2.1		
ZrII(95)	5112.27	0.89	-1.9	0.62	82.7
LaII(36)	5114.55	0.91:		0.82	81.6:
C ₂ (0;0)R1(25)	5116.66			0.93	77.7
C ₂ (0;0)R3(23)	5116.89			0.95	77.6
CeII	5117.18	0.97		0.90	81.4:
YII(20)	5119.12	0.88	-2.1	0.69	80.9:
FeII(35)	5120.34	0.80	-1.0:	0.91	82.7
C ₂ (0;0)R1(23)	5121.44			0.93	77.3
C ₂ (0;0)R3(21)	5121.69			0.94	77.7
LaII(36)	5123.00				
YII(21)	5123.22	0.70		0.53	
C ₂ (0;0)R1(22)	5123.79				77.3:
C ₂ (0;0)R3(20)	5124.04				77.3:
C ₂ (0;0)R1(21)	5125.98			0.91	77.5
C ₂ (0;0)R3(19)	5126.26			0.93	77.5
C ₂ (0;0)R3(20)	5128.19			0.90	77.3
C ₂ (0;0)R3(18)	5128.49			0.93	77.9
TiII(86)	5129.16	0.50			
C ₂ (0;0)R1(19)	5130.27			0.89	77.9

Element	λ Å	α Per		HD 56126	
		r	V_r	r	V_r
C ₂ (0;0)R1(18)	5132.36			0.86	77.7
FeII(35)	5132.66	0.77	-2.6:		82.2:
FeI(1092)	5133.69	0.64	-2.0	0.88	82.9
C ₂ (0;0)R1(17)	5134.32			0.89	77.1
C ₂ (0;0)R3(15)	5134.67			0.91	77.4
C ₂ (0;0)R1(16)	5136.27			0.89	77.6
C ₂ (0;0)R2(15)	5136.44			0.94	77.7
C ₂ (0;0)R3(14)	5136.66			0.89	77.7
C ₂ (0;0)R1(15)	5138.11			0.89	77.3
C ₂ (0;0)R2(14)	5138.32			0.93	77.1
C ₂ (0;0)R3(13)	5138.51			0.90	77.6
C ₂ (0;0)R1(14)	5139.93			0.88	77.5
C ₂ (0;0)R2(13)	5140.14			0.92	77.8
C ₂ (0;0)R3(12)	5140.38			0.89	77.6
C ₂ (0;0)R1(13)	5141.65			0.87	77.2
C ₂ (0;0)R2(12)	5141.90			0.89	77.1
C ₂ (0;0)R3(11)	5142.11			0.89	77.7
C ₂ (0;0)R1(12)	5143.33			0.86	77.6
C ₂ (0;0)R2(11)	5143.60			0.89	77.4
C ₂ (0;0)R3(10)	5143.86			0.88	77.7
C ₂ (0;0)R1(11)	5144.92			0.85	77.5
C ₂ (0;0)R2(10)	5145.23			0.87	77.6
C ₂ (0;0)R3(09)	5145.48			0.87	77.5
FeII(35)	5146.11	0.73:		0.86	83.1:
C ₂ (0;0)R1(10)	5146.46			0.83	77.5
C ₂ (0;0)R2(09)	5146.81			0.88	77.6
C ₂ (0;0)R3(08)	5146.12			0.88	77.2
C ₂ (0;0)R1(09)	5147.93			0.84	77.4
C ₂ (0;0)R2(08)	5148.33			0.83	77.0
C ₂ (0;0)R3(07)	5148.61			0.84	77.3
C ₂ (0;0)R1(08)	5149.33			0.84	77.8
C ₂ (0;0)R2(07)	5149.79			0.85	77.1
C ₂ (0;0)R3(06)	5150.14			0.86	77.6
FeI(16)	5150.85	0.70	-0.9:		
C ₂ (0;0)R2(06)	5151.17			0.83	77.3
C ₂ (0;0)R2(05)	5152.52			0.81	77.0
C ₂ (0;0)R2(04)	5153.77			0.74	77.2
TiII(70)	5154.07	0.51		0.57:	
C ₂ (0;0)R2(03)	5154.99			0.82	77.4
C ₂ (0;0)R1(02)	5156.11			0.77	77.2
C ₂ (0;0)R2(01)	5157.16			0.86	77.8
C ₂ (0;0)P2(04)	5161.98			0.75	76.6
FeI(1089)	5162.27	0.66	-1.6		
C ₂ (0;0)P2(05)	5162.58			0.66	77.3
C ₂ (0;0)P2(07)	5163.13			0.75	77.4
C ₂ (0;0)P1(14)	5165.03			0.56	78.0
C ₂ (0;0) head	5165.24			0.72:	
MgI(2)	5167.32	0.30		0.55	
FeI(37)	5167.49				

Element	λ Å	α Per		HD 56126	
		r	V_r	r	V_r
FeII(42)	5169.03	0.27	-2.7	0.56: 0.33	77.0: 97.4
FeI(36)	5171.60	0.56	-1.7	0.88	82.6
MgI(2)	5172.68	0.37	-1.4	0.51	82.7
NdII	5179.78			0.94	81.6
FeI(1166)	5180.07	0.92			
MgI(2)	5183.60	0.32	-2.1	0.45	81.6
TiII(86)	5185.91	0.54	-2.1	0.69	82.0
CeII(46)	5187.46	0.93:		0.81	81.4
TiII(70)	5188.69	0.41		0.57	
CaI(49)	5188.85				
FeI(383)	5191.45	0.56			
FeII(52)	5191.58			0.58	82.8:
FeI(383)	5192.35	0.57		0.83:	
NdII(75)	5192.61			0.81:	
YII(28)	5196.43			0.75	81.8
FeII(49)	5197.58	0.46	-2.4	0.59	83.3
YII(20)	5200.41	0.70	-2.8:	0.61	83.7:
FeI(66)	5202.34	0.67		0.94	81.4
YII(20)	5205.73			0.55	84.8:
CrI(7)	5206.04	0.42			
TiII(103)	5211.54	0.72	-2.7	0.83	82.3
NdII(44)	5212.37	0.96	-2.0:	0.95	81.1
FeII	5216.85			0.94	82.2
PrII(35)	5220.11			0.94	82.0
TiII(70)	5226.54				
FeI(383)	5226.87	0.37:	-1.9:	0.60	83.6:
FeI(37)	5227.19			0.79	81.6
FeI(1091)	5228.38	0.89			
NdII(46)	5228.43				
FeI(553)	5229.85	0.74	-1.3	0.95	82.8
FeII(49)	5234.63	0.45	-2.3	0.57	83.8
CrII(43)	5237.32	0.60	-1.9	0.68	82.7:
ScII(26)	5239.82	0.66	-1.8	0.76	82.4
CrII(23)	5246.77	0.80:		0.91	83.1
FeII(49)	5254.93	0.62	-1.3	0.74	82.0
NdII(43)	5255.51			0.91	81.6:
FeII(41)	5256.93	0.80	-1.7	0.89	83.2
FeII	5260.26	0.92:		0.90	81.9:
TiII(70)	5262.11	0.33:		0.81	
CaI(22)	5262.24				
FeII(48)	5264.81	0.60	-2.0	0.56	87.4:
FeI(383)	5266.55	0.58	-1.8	0.88	82.3
TiII(103)	5268.62	0.73:		0.86:	83.0:
FeI(15)	5269.54	0.42	-2.0	0.70	82.1
FeII(185)	5272.39	0.86		0.91	83.3:
CeII(15)	5274.23	0.92:		0.80	81.9
CrII(43)	5274.98	0.60:		0.71	82.9
FeII(49)	5276.00	0.42	-3.0	0.56	84.8

Element	λ Å	α Per		HD 56126	
		r	V_r	r	V_r
FeI(383)	5281.79	0.70	-2.1	0.95	81.3
FeII(41)	5284.10	0.53:		0.68	83.1
YII(20)	5289.82	0.95	-2.3	0.87	81.2
LaII(6)	5290.83	0.96	-1.8:	0.93	81.1:
NdII(75)	5293.16	0.90	-1.4	0.84	82.2
HfII(49)	5298.06			0.94	82.7:
CrII(24)	5305.86	0.76	-1.5	0.84	82.9
CrII(43)	5308.43	0.79	-2.1	0.85	82.7
CrII(43)	5310.69	0.84:		0.92	82.7
CrII(43)	5313.58	0.70	-1.6	0.78	82.9
FeII(49,48)	5316.66	0.34	-1.3:	0.48	88.0:
ScII(22)	5318.35	0.85	-1.4	0.95	83.2:
NdII(75)	5319.82	0.92:		0.85	81.5
YII(20)	5320.78			0.94	82.0
FeI(553)	5324.18	0.58	-2.4	0.81	82.6
FeII(49)	5325.56	0.65	-2.5	0.73	82.6
FeI(15)	5328.04	0.37:		0.74	82.4
OI(12)	5328.69			0.93	83.3
CrII(43)	5334.87	0.72	-2.1	0.80	82.9
TiII(69)	5336.79	0.55	-2.2	0.71	81.9
FeII(48)	5337.73	0.71			
CrII(43)	5337.79			0.81	
FeI(37)	5341.02	0.61	-1.6	0.94	81.5
ZrII(115)	5350.09				
ZrII(115)	5350.35	0.87:		0.64	
FeI(1062)	5353.38	0.79:			
CeII(15)	5353.53			0.79	81.3
FeII(48)	5362.86	0.51	-1.9	0.63	83.5
FeI(1146)	5364.87	0.72		0.93	82.6
FeI(1146)	5367.47	0.70	-2.1	0.90	82.4
CrII(29)	5369.35			0.96	82.2
FeI(1146)	5369.96	0.65	-2.1	0.88	82.9
FeI(15)	5371.49	0.46	-2.2	0.82	81.8
NdII(79)	5371.92			0.92	81.5:
LaII(95)	5377.05			0.94	82.3
Cl(11)	5380.34	0.85:	-1.9:	0.68	81.9
TiII(69)	5381.03	0.63	-2.8	0.78	81.8
FeI(1146)	5383.37	0.63	-2.2	0.86	82.6
FeI(553)	5393.17	0.71			
CeII(24)	5393.39			0.81	
FeI(553)	5393.17	0.71			
CeII(24)	5393.39			0.81	
FeI(15)	5397.13	0.52	-2.1	0.89	81.6
YII(35)	5402.78	0.85	-2.1	0.59	81.9
FeI(1145)	5404.14	0.59		0.87	82.2
FeI(15)	5405.77	0.50	-1.9	0.89	81.4
CeII(23)	5409.22			0.90	81.4
FeI(1165)	5410.91	0.70	-1.5	0.91	82.8:
FeII(48)	5414.07	0.74	-2.2	0.84	82.5

Element	λ Å	α Per		HD 56126	
		r	V_r	r	V_r
FeI(1165)	5415.20	0.64	-2.1	0.87	82.2
ZrII(94)	5418.01			0.96	80.6:
TiII(69)	5418.77	0.67	-2.0	0.82	82.4
CrII(23)	5420.93	0.79		0.90	83.0
FeI(1146)	5424.07	0.60	-1.8	0.84	82.7
FeII(49)	5425.25	0.67	-2.0	0.75	82.7
FeII	5427.80	0.94	-1.4	0.96	81.4:
FeI(15)	5434.52	0.56	-1.8	0.91	81.8
OI(11)	5435.18			0.97	
OI(11)	5435.78			0.97	82.4
OI(11)	5436.86			0.95:	
NdII(76)	5442.29			0.97	81.0:
FeI(1163)	5445.04	0.74	-1.9	0.95	82.1
FeI(15)	5446.92	0.48		0.89	81.0:
NdII	5451.12	0.97:		0.96	81.5:
CeII(24)	5468.38	0.96		0.92	89.5
CeII(24)	5472.30			0.90	89.0
YII(27)	5473.39	0.87:		0.66	90.0
ZrII(115)	5477.79			0.89	89.7
CrII(50)	5478.37	0.76	-1.7	0.83	89.3
YII(27)	5480.74	0.83:		0.66	90.0
NdII(79)	5485.71	0.97	-1.3:	0.92	90.3:
TiII(68)	5490.68	0.82	-1.2:	0.93	90.4:
YII(27)	5497.41	0.62		0.51	90.5
FeI(15)	5497.52				
FeI(15)	5501.47	0.72			
CrII(50)	5502.08	0.80	-2.7:	0.87	90.2
FeI(15)	5506.79	0.67	-0.9:	0.96	90.3:
CrII(50)	5508.62	0.82	-2.9:	0.89	89.0:
YII(19)	5509.90	0.80	-1.4	0.65	90.9:
CrII(23)	5510.71	0.83	-1.9	0.90	90.7:
YII(27)	5521.56	0.92	-2.1	0.69	90.3
ScII(31)	5526.81	0.55	-2.1	0.60	90.4
MgI(9)	5528.41	0.58	-2.4	0.76	88.7
FeII(55)	5534.84	0.57	-1.8	0.63	90.0
FeI(926)	5543.19	0.90	-2.1	0.97	89.8
FeI(1062)	5543.94	0.89	-2.4	0.96	89.0:
YII(27)	5544.61	0.89:		0.65	91.0
CI	5545.07	0.92:		0.82:	88.0:
YII(27)	5546.01	0.90:		0.66	90.1
CI	5547.27			0.95	89.5
CI	5551.03			0.95	87.8:
CI	5551.59			0.92	88.5
FeI(1183)	5554.90	0.84	-2.7	0.95	90.8:
FeI(686)	5569.62	0.71	-1.8	0.93	89.0
FeI(686)	5572.84	0.63		0.89	90.0
FeI(686)	5586.76	0.61	-1.4	0.84	89.2
CaI(21)	5588.76	0.65	-2.0	0.90	88.8
CaI(21)	5594.47	0.66:		0.89	88.4

Element	λ Å	α Per		HD 56126	
		r	V_r	r	V_r
CaI(21)	5601.28	0.80	-2.9	0.97	88.7
CeII(26)	5610.26	0.97:			
YII(19)	5610.36			0.93	
FeI(686)	5615.64	0.57		0.82	89.5
NdII(86)	5620.65			0.93	88.5
FeI(686)	5624.54	0.75	-2.4	0.93	90.2:
FeII(57)	5627.49	0.87	-1.6	0.93	90.3
Cl	5629.93	0.98:	-1.5:	0.96	88.5
FeI(1314)	5633.95	0.89	-2.0		
FeI(1087)	5638.27	0.87	-2.3		
ScII(29)	5640.98	0.73		0.82	90.6
ScII(29)	5657.87	0.56:		0.72	90.3
ScII(29)	5658.34			0.83:	88.5
FeI(1087)	5662.52				
YII(38)	5662.94	0.66:		0.42	90.6
ScII(29)	5667.15	0.77	-1.3	0.87	90.0
Cl	5668.95			0.72	90.4
ScII(29)	5669.03	0.72	-2.9		
LaII(95)	5671.54			0.96	91.2:
NaI(6)	5682.64	0.79:		0.96	88.8:
ScII(29)	5684.19	0.70:		0.83	90.5
NaI(6)	5688.21	0.72	-0.9:	0.92	91.2:
NdII(79)	5688.54			0.91	89.6:
Cl	5693.11	0.98:		0.94	89.5
MgI(8)	5711.09	0.85	-1.6	0.98:	
NiI(231)	5715.09	0.90	-1.6		
Cl	5720.78			0.98	89.5:
YII(34)	5728.89	0.94	-1.9	0.75	90.3
FeI(1087)	5731.77	0.92	-2.1	0.98	
FeII(57)	5732.72	0.94		0.97	90.0
FeI(1180)	5752.04	0.93	-2.2		
FeI(1107)	5763.00	0.80	-3.0:	0.96:	89.3:
LaII(70)	5769.06	0.96	-1.2:	0.86	88.9
SiI(17)	5772.15	0.91	-1.8	0.98:	
FeI(1087)	5775.08	0.93	-1.7		
YII(34)	5781.69			0.84	90.5
Cl	5793.12	0.89		0.87	88.9
Cl	5794.46			0.97	90.6:
LaII(4)	5797.59			0.87	89.9
SiI(9)	5797.86	0.90			
Cl	5800.59	0.95:		0.91	89.2
NdII(79)	5804.02			0.93	90.5
Cl	5805.19	0.94:		0.94	90.5
LaII(4)	5805.78	0.94	-2.7:	0.86	89.9
FeI(1180)	5806.73	0.93	-2.2	0.98	90.2
LaII(4)	5808.31	0.98:		0.97	91.5:
FeI(982)	5809.22	0.95	-1.3	0.98:	
VII(99)	5819.93	0.95	-1.4	0.98:	90.0:
FeII(164)	5823.15	0.96	-2.5:	0.97	89.6:

Element	λ Å	α Per		HD 56126	
		r	V_r	r	V_r
NdII(86)	5842.39	0.99:		0.96	88.3:
FeI(1178)	5852.22	0.96	-1.8		
BaII(2)	5853.68	0.63	-2.1	0.53	90.8
CaI(47)	5857.45	0.72		0.94	88.9
FeI(1180)	5862.36	0.85	-1.9	0.96	88.8
LaII(62)	5863.70	0.98		0.97	89.8
LaII(35)	5880.63			0.96	90.7:
NaI(1)	5889.95	0.45:	-1.2:	0.21	13.0
		0.05	+2.2	0.32	24.0
				0.37	31.4
				0.10	75.7
				0.40	89.0
NaI(1)	5895.92	0.50:	-0.9:	0.38	13.2
		0.06	+2.3	0.51	24.7
				0.48	32.0
				0.16	76.3
				0.45	89.8
FeI(982)	5934.66	0.89	-2.2		
SiI(16)	5948.54	0.83	-3.0	0.97:	
SiII(4)	5957.56			0.93	88.0:
CeII(80)	5975.83			0.94	89.9
SiII(4)	5978.93			0.88	87.5
FeI(1175)	5983.68	0.89	-0.7	0.95:	89.0:
FeI(1260)	5984.82	0.86	-1.9	0.96:	88.0:
FeII(46)	5991.37	0.75	-1.7	0.84	90.3
Cl	6001.13	0.98:		0.92	89.5
Cl	6002.98			0.95	89.7:
FeI(959)	6003.02	0.88	-2.4		
Cl	6006.03	0.96:		0.86	89.5
Cl	6010.68	0.98	-1.2	0.92	88.8
Cl	6012.24	0.98:	-1.5:	0.94	90.3:
Cl	6013.32			0.80	87.7:
MnI(27)	6013.49	0.89:			
Cl	6016.45			0.93	89.2:
MnI(27)	6016.64	0.91:	-2.0:		
MnI(27)	6021.80	0.90	-2.0:		
FeI(1178)	6024.07	0.82	-2.2	0.94	88.8
ZrII(136)	6028.64	0.97:		0.91	89.1
CeII(30)	6034.20	0.98	-1.7	0.96	90.8:
CeII(30)	6043.40	0.99	-1.5:	0.94	89.7
FeI(207)	6065.49	0.81	-1.4	0.98:	
FeII(46)	6084.10	0.83	-1.5	0.90	
ZrII(106)	6106.47	0.97:		0.93	90.9
FeII(46)	6113.32	0.88	-1.6	0.93	88.6
ZrII(93)	6114.78	0.98	-1.5:	0.92	92.2:
Cl	6120.82	0.99:		0.97	89.8
CaI(3)	6122.22	0.69	-0.9	0.93	89.5
FeI(169)	6136.62	0.75		0.95	89.0:
FeI(207)	6137.70	0.78	-2.0	0.96	89.2:

Element	λ Å	α Per		HD 56126	
		r	V_r	r	V_r
BaII(2)	6141.72	0.56	-1.4	0.37	92.3
FeII(74)	6147.74	0.74	-1.4	0.77	90.2
FeII(74)	6149.25	0.75	-1.5	0.77	90.0
SiII(29)	6155.98	0.89			
OI(10)	6155.98	0.95:		0.82	87.0:
OI(10)	6156.17	0.95:		0.82	87.1
OI(10)	6158.18			0.79	88.0
FeI(1260)	6170.51	0.90	-1.5	0.97	89.7
FeII(200)	6175.14			0.95	90.2
LuII(2)	6221.88	0.98:		0.90	89.9:
FeII(74)	6238.39	0.74	-1.7	0.76	90.0
SeII(28)	6245.62	0.80:	-0.5:	0.90	90.0:
FeII(74)	6247.56	0.66	-2.2	0.70	89.9:
FeII	6248.90	0.94	-1.4	0.94	89.3
FeI(169)	6252.56	0.81	-1.9	0.97	89.5
LaII(33)	6262.30	0.96	-0.6:	0.89	90.2
FeII	6317.99	0.81	-1.0:	0.86	88.8:
FeI(168)	6318.03				
SiII(2)	6347.10	0.65	-2.0	0.51	89.7
FeII(40)	6369.46	0.84	-1.6	0.91	90.5
SiII(2)	6371.36	0.72	-1.8	0.57	89.5
FeII	6383.72	0.91	-1.6	0.92	89.8
FeII	6385.46	0.93	-2.0	0.94	88.4:
LaII(33)	6390.49	0.97		0.89	90.3
FeI(168)	6393.61	0.79	-2.5	0.96	90.5:
Cl	6397.98	0.98:		0.94	89.2
FeII(74)	6416.92	0.75	-1.0	0.80	90.2
FeI(62)	6430.85	0.83	-1.6	0.97	90.6:
FeII(40)	6432.68	0.75	-1.4	0.81	90.0
CaI(18)	6439.08	0.69	-1.6	0.89	90.0
FeII	6442.95	0.95	-1.2	0.95	88.9
FeII(199)	6446.41	0.95	-1.2	0.95	91.1:
OI(9)	6453.60	0.97:		0.94	87.9
OI(9)	6454.45	0.98:	-2.0:	0.94	88.0
FeII(74)	6456.39	0.60	-0.2:	0.66	91.0:
TiII(91)	6491.57	0.78:		0.91	90.7:
BaII(2)	6496.91	0.55		0.52	
FeII(40)	6516.08	0.66	-2.0	0.77	90.2
LaII(33)	6526.99			0.91	90.7:
MgII(23)	6545.97			0.93	89.8
FeI(268)	6546.25	0.92:			
H α	6562.81	0.19	-2.1	0.32	58.0
				0.40:	74.0:
				0.89	82.8:
Cl(22)	6587.61	0.89	-1.7	0.72	89.5
SeII(19)	6604.59	0.89		0.94	91.1:
TiII(91)	6606.95	0.95	-2.2:	0.96	89.5
Cl	6611.35			0.96	90.6:
YII	6613.75	0.91		0.73	90.0

Element	λ Å	α Per		HD 56126	
		r	V_r	r	V_r
Cl	6654.61			0.94	89.5:
Cl	6655.51			0.91	90.5
YII(26)	6795.42			0.88	90.0
Cl	7087.83			0.90	89.3
Cl	7100.12			0.91	89.7
SiI(23)	7415.95			0.95:	87.5:
SiI(23)	7423.50			0.92	91.0:
EuII(8)	7426.57			0.93:	85.0:
Cl	7476.18			0.89:	86.0:
Cl	7483.44			0.90	85.0:
LaII(1)	7483.48				
FeI(1077)	7511.03			0.97:	87.0
KI(1)	7664.91			0.83	77.5
OI(1)	7771.94			0.34	93.5
OI(1)	7774.17			0.35	94.8:
OI(1)	7775.39			0.42:	
Cl	7860.89			0.91:	88.0:
MgII(8)	7877.05			0.89	90.5:
YII(32)	7881.90			0.89	90.5:
MgII(8)	7896.37			0.80	88.7:
H(P27)	8306.12			0.91:	91.0:
H(P25)	8323.43			0.91:	91.0:
H(P20)	8392.40			0.64	87.0:
H(P19)	8413.32			0.62	88.0:
H(P18)	8437.96			0.60	92.0:
OI(4)	8446.5:			0.26	94.0:
H(P17)	8467.25			0.58	93.0:
CaII(2)	8542.11			0.40	85.0:
H(P15)	8545.38			0.53	94.0:
NI(8)	8567.74			0.90	89.0:
NI(8)	8594.01				90.0:
H(P14)	8598.39			0.49	93.0:
NI(8)	8629.24			0.78:	88.0:
NI(1)	8703.25			0.85:	90.0:
NI(1)	8711.70			0.83	87.0:
NI(1)	8718.83			0.84	89.0:
H(P12)	8750.47			0.43	98.0: